

2

DTIC FILE COPY

USA-CERL TECHNICAL MANUSCRIPT N-89/01
November 1988



**US Army Corps
of Engineers**
Construction Engineering
Research Laboratory

AD-A203 148

Attenuation of Blast Waves Using Foam and Other Materials

by
Richard Raspet
S. K. Griffiths
Joseph M. Powers
Herman Krier
Timothy D. Panczak
P. Barry Butler
F. Jahani

Noise is a problem everywhere the Army trains or tests with large weapons or helicopters. The Army Environmental Office and the Secretary of the Army have listed noise and hazardous waste as the major problems facing the Army into the 21st century.

Research at the U.S. Army Construction Engineering Research Laboratory (USA-CERL) is aimed at solving the total noise problem for the Army. This report documents several years of fundamental research into methods to quiet explosive noise and materials used to reduce the noise from explosions.

Articles regarding this USA-CERL research have been published in different journals around the world. These articles are reproduced here in chronological order.

Approved for public release; distribution is unlimited.

DTIC
ELECTE
30 JAN 1989
S D
E

89 1 30 109

UNCLASSIFIED

SECURITY CLASSIFICATION OF THIS PAGE

| REPORT DOCUMENTATION PAGE | | | | Form Approved OMB No 0704-0188 Exp Date Jun 30, 1985 | |
|--|-------|--|---|--|-------------------------|
| 1a REPORT SECURITY CLASSIFICATION UNCLASSIFIED | | 1b RESTRICTIVE MARKINGS | | | |
| 2a SECURITY CLASSIFICATION AUTHORITY | | 3 DISTRIBUTION/AVAILABILITY OF REPORT Approved for public release; distribution is unlimited. | | | |
| 2b DECLASSIFICATION/DOWNGRADING SCHEDULE | | | | | |
| 4 PERFORMING ORGANIZATION REPORT NUMBER(S) USA-CERL TM N-89/01 | | 5 MONITORING ORGANIZATION REPORT NUMBER(S) | | | |
| 6a NAME OF PERFORMING ORGANIZATION U.S. Army Construction Engr Research Laboratory | | 6b. OFFICE SYMBOL (if applicable) CECER-EN | 7a NAME OF MONITORING ORGANIZATION | | |
| 6c. ADDRESS (City, State, and ZIP Code) P.O. Box 4005 Champaign, IL 61820-1305 | | 7b. ADDRESS (City, State, and ZIP Code) | | | |
| 8a. NAME OF FUNDING/SPONSORING ORGANIZATION | | 8b OFFICE SYMBOL (if applicable) | 9. PROCUREMENT INSTRUMENT IDENTIFICATION NUMBER | | |
| 8c. ADDRESS (City, State, and ZIP Code) | | 10. SOURCE OF FUNDING NUMBERS | | | |
| | | PROGRAM ELEMENT NO. | PROJECT NO. | TASK NO. | WORK UNIT ACCESSION NO. |
| 11 TITLE (Include Security Classification) "Attenuation of Blast Waves Using Foam and Other Materials" (Unclassified) | | | | | |
| 12 PERSONAL AUTHOR(S) Raspert, Richard; Griffiths, S. K.; Powers, Joseph M.; Krier, Herman; Panczak, Timothy D.; Butler, P. Barry; and Jahani, F. | | | | | |
| 13a TYPE OF REPORT Final | | 13b TIME COVERED FROM _____ TO _____ | 14 DATE OF REPORT (Year, Month, Day) 1988 November | | 15. PAGE COUNT 73 |
| 16 SUPPLEMENTARY NOTATION Copies are available from the National Technical Information Service Springfield, VA 22161 | | | | | |
| 17 COSATI CODES | | 18 SUBJECT TERMS (Continue on reverse if necessary and identify by block number) | | | |
| FIELD | GROUP | SUB-GROUP | noise reduction; reprints, (cdc) ← | | |
| 24 | 02 | | blast noise; foam; Army research. | | |
| 19 ABSTRACT (Continue on reverse if necessary and identify by block number) <i>(have been listed)</i> Noise is a problem everywhere the Army trains or tests with large weapons or helicopters. The Army Environmental Office and the Secretary of the Army have listed noise and hazardous waste as the major problems facing the Army into the 21st century. Research at the U.S. Army Construction Engineering Research Laboratory (USA-CERL) is aimed at solving the total noise problem for the Army. This report documents several years of fundamental research into methods to quiet explosive noise and materials used to reduce the noise from explosions. <i>This report reproduces journal articles.</i> Articles regarding this USA-CERL research have been published in different journals around the world. These articles are reproduced here in chronological order. <i>Keywords!</i> | | | | | |
| 20 DISTRIBUTION/AVAILABILITY OF ABSTRACT <input type="checkbox"/> UNCLASSIFIED/UNLIMITED <input checked="" type="checkbox"/> SAME AS RPT <input type="checkbox"/> DTIC USERS | | | 21 ABSTRACT SECURITY CLASSIFICATION UNCLASSIFIED | | |
| 22a NAME OF RESPONSIBLE INDIVIDUAL LINDA WHEATLEY | | 22b TELEPHONE (Include Area Code) (217)352-6511 (ext. 343) | | 22c OFFICE SYMBOL CECER-IMT | |

DD FORM 1473, 84 MAR

83 APR edition may be used until exhausted
All other editions are obsoleteSECURITY CLASSIFICATION OF THIS PAGE
UNCLASSIFIED

A

FOREWORD

This material was compiled with the support of the Environmental Division (EN) of the U.S. Army Construction Engineering Research Laboratory (USA-CERL). Dr. R. K. Jain is Chief, USA-CERL-EN, and Dr. Paul D. Schomer is Team Leader for the Acoustics Team, USA-CERL-EN.

COL Carl O. Magnell is Commander and Director of USA-CERL, and Dr. L. R. Shaffer is Technical Director.

| | |
|----------------------|-------------------------------------|
| Accession For | |
| NTIS GRA&I | <input checked="" type="checkbox"/> |
| DTIC TAB | <input checked="" type="checkbox"/> |
| Unannounced | <input type="checkbox"/> |
| Justification | |
| By _____ | |
| Distribution/ | |
| Availability Codes | |
| Dist | Avail and/or Special |
| A-1 | |

QUALITY INSPECTOR
1

CONTENTS

| | Page |
|--|------|
| DD FORM 1473 | 1 |
| FOREWORD | 3 |
| INTRODUCTION | 5 |
| THE REDUCTION OF BLAST NOISE WITH AQUEOUS FOAM. Richard Raspet, U.S. Army Construction Engineering Research Laboratory, S. K. Griffiths, Sandia National Laboratories | 6 |
| ATTENUATION OF BLAST WAVES WHEN DETONATING EXPLOSIVES INSIDE BARRIERS. Joseph M. Powers and Herman Krier, University of Illinois | 13 |
| SHOCK PROPAGATION AND BLAST ATTENUATION THROUGH AQUEOUS FOAMS. Timothy D. Panczak and Herman Krier, University of Illinois, and P. Barry Butler, University of Iowa | 26 |
| THE EFFECT OF MATERIAL PROPERTIES ON REDUCING INTERMEDIATE BLAST NOISE. R. Raspet, U.S. Army Construction Engineering Research Laboratory, and P. B. Butler and F. Jahani, University of Iowa | 42 |
| THE REDUCTION OF BLAST OVERPRESSURES FROM AQUEOUS FOAM IN A RIGID CONFINEMENT. R. Raspet, U.S. Army Construction Engineering Research Laboratory, and P. B. Butler and F. Jahani, University of Iowa | 60 |
| DISTRIBUTION | |

ATTENUATION OF BLAST WAVES USING FOAM AND OTHER MATERIALS

INTRODUCTION

Noise is a problem everywhere the Army trains or tests with large weapons or helicopters. The Army Environmental Office, the U.S. Army Construction Engineering Research Laboratory (USA-CERL), and the U.S. Army Environmental Hygiene Agency (USAEHA) have compiled a list of about 50 installations where training or testing has been altered or curtailed because of off-post noise problems. For these and other reasons, the Army Environmental Office and the Secretary of the Army have listed noise and hazardous waste as the two major problems facing the Army through the year 2000 and beyond. Moreover, these noise sources are unique to the Army and ones for which technological solutions are for the most part lacking. For U.S. Army Europe (USAREUR), noise is an even bigger problem than in the United States.

In general, USA-CERL research is aimed at solving the total noise problem for the Army. This includes noise prediction, mitigation, measurement and monitoring, and management. This report is a compilation of articles on noise mitigation, in particular materials to quiet explosive noise. The articles, which have been published in reviewed scientific journals around the world, document several years of fundamental research by the USA-CERL acoustics team. They are reprinted here in chronological order.

The reduction of blast noise with aqueous foam

Richard Raspet

U.S. Army Construction Engineering Research Laboratory, P.O. Box 4005, Champaign, Illinois 61820

S. K. Griffiths

Sandia National Laboratories, P.O. Box 5800, Albuquerque, New Mexico 87185

(Received 20 August 1981; accepted for publication 29 August 1983)

Experiments were performed to investigate the potential of water-based foams to reduce the farfield noise levels produced by demolitions activity. Measurements of the noise reductions in flat-weighted sound exposure level (FSEL), C-weighted sound exposure level (CSEL), and peak level were made for a variety of charge masses, foam depths, and foam densities (250:1 and 30:1 expansion ratio foams). Scaling laws were developed to relate the foam depth, foam density, and charge mass to noise reductions. These laws provide consistent results for reductions in the peak level, FSEL and CSEL up to a dimensionless foam depth of 2.5. A two part model for the mechanisms of sound level reductions by foam is suggested.

FACS numbers: 43.50.Gf, 43.28.Mw

INTRODUCTION

To date, most research into mitigating demolition effects has concentrated on nearfield phenomena, particularly the damaging effects of the blastwave (the nearfield is the region within a few hundred explosive charge radii of the explosive). Little has been done to measure and evaluate blast effects in the farfield, but it is the farfield effects of blasts which are becoming a serious environmental issue, i.e., annoyance and damage complaints from individuals and communities subjected to increased environmental noise levels can restrict, or eliminate, blast producing activities.

To address this problem of the farfield effects of demolition (and related activities), we have considered several methods of reducing blast noise, including the use of water-based foams as a mitigating agent. This paper describes an experimental investigation into the use of both low and high density aqueous foams to quiet blast noise in the farfield. The data is used to develop scaling laws for the foam so that the level of noise reduction can be predicted for various amounts and densities of foams. We also discuss past nearfield investigations when they can be related to our farfield measurements. Finally, a two mechanism model for the reduction of sound levels by foam is proposed.

1. METHOD

Two test series were performed using different expansion ratio foams. The expansion ratio is the ratio of foam volume to liquid content volume. To simplify the data analysis, simple lightweight cubical or near cubical foam enclosures were used. For all but the initial tests, these enclosures were constructed of a wooden frame with polyethylene sheeting for the walls. The charges were centered in the cube on crushable plastic posts (Fig. 1). Spheres of Composition Four (C-4) plastic explosive were used in all tests. During all tests, the charges were set in pairs: a test charge under foam and a reference charge without foam. For cases where the enclosure was slightly noncubical, the geometrically aver-

aged foam depth was used in the data analysis

$$d = \sqrt[3]{l \times w \times h} \quad (1)$$

where l , w , and h are the foam dimensions in meters.

In all tests, the flat-weighted sound exposure level (FSEL), C-weighted sound exposure level (CSEL), and the peak level were measured at four microphone positions, two each on opposite sides of the explosive. The standard microphone distances used in most tests were 60 and 120 m (Fig. 2). Two trials were performed for each configuration. The levels were read using a True Integrating Environmental Noise Monitor and Sound Exposure Level Meter, designed and constructed by the U.S. Army Construction Engineering Research Laboratory. The signals were recorded for later analysis on an AMPEX 2230 14-track FM recorder. The peak level, defined as

$$20 \log(p/p_0),$$

where $p_0 = 20 \mu\text{Pa}$, is commonly used to identify excessive noise levels around explosive facilities and to identify when the possibility of structural damage exists. The sound expo-

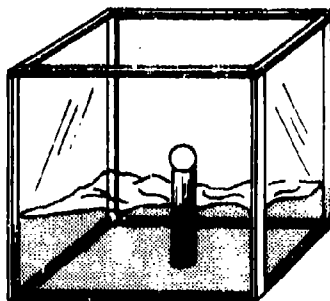


FIG. 1. Experimental setup for unconfined explosive test.

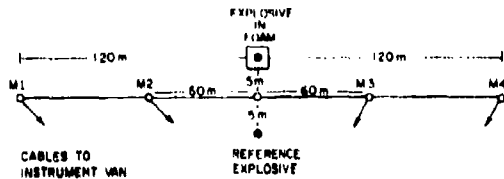


FIG. 2. Microphone positions for foam tests.

sure level (SEL) is defined as

$$10 \log \left(\int p^2 dt / p_0^2 t_0 \right),$$

where p_0 is defined above, $t_0 = 1.0$ s and the integral is performed over the entire duration of the transient. The FSEL is performed with no frequency weighting, the C-weighted SEL with a standard C-weighting filter in the system before the integration is performed.

The CSEL is important for the environmental assessment of blast noise since it can be used to calculate the C-weighted average day/night level (CDNL). The CDNL is recommended by the Committee on Hearing, Bioacoustics, and Biomechanics of the National Research Council¹ to assess the environmental impacts of high-energy impulsive noise and is used by the Department of Defense to assess blast noise.²

II. SERIES 1: HIGH EXPANSION FOAM

The first series of tests investigated the noise reducing properties of high expansion foam. The foam was made with a National Foam System WP-25 generator using National's 1% High Expansion Foam solution. When water is provided (by a fire truck) at 1400-1700 kPa, this generator produces foam with a nominal 250:1 expansion ratio. The expansion ratio varies slowly with time, but samples taken 30 s after generation were usually within 20% of the nominal value. The individual bubbles were approximately 1 cm in diameter. This type of foam was stable and usable for 10-15 min after generation in low wind conditions.

A. Test 1

The first test was a feasibility test. Two charge sizes and two foam configurations were used. In one case, the charges were set in a 3.0 m × 3.0 m × 1.85 m pit; the foam in the pit was piled about 0.30 m above ground level. In this partially confined case, the reductions in all noise metrics were about 14 dB for the 0.57-kg charge, and about 9 dB for the 2.37-kg charge.

The second configuration was an enclosure 2.4 × 2.4 × 1.7 m high, constructed as described in Sec. I. This enclosure produced reductions of about 10 and 5 dB in all metrics (peak level, FSEL, CSEL) for the 0.57- and 2.37-kg charges, respectively.

The results of test 1 established that significant environmental noise reductions could be achieved. These reductions were similar for all metrics measured, but did not provide

enough information to allow foam thickness and charge size to be related to the reduction in sound levels.

B. Test 2

Test 2 investigated the dependence of CSEL, FSEL, and peak level on foam depth for two charge masses. The enclosure dimensions varied from 0.30 m to 1.5 m in 0.30-m steps. Charges masses of 0.57 and 0.061 kg were used. Plots of foam depth versus reduction for all three metrics were linear within the accuracy of the data. The data, along with those for tests 3 and 4, for the test are displayed in Fig. 3 ($\Delta = 0.061$ kg, $\circ = 0.57$ kg) as reductions in CSEL, FSEL, and peak level versus the cube root scaled foam depth. The results of these six experiments show that all three sound levels are reduced linearly up to the largest scaled foam depth, approximately 2.9 m/kg^{1/3}. At that depth, the reduc-

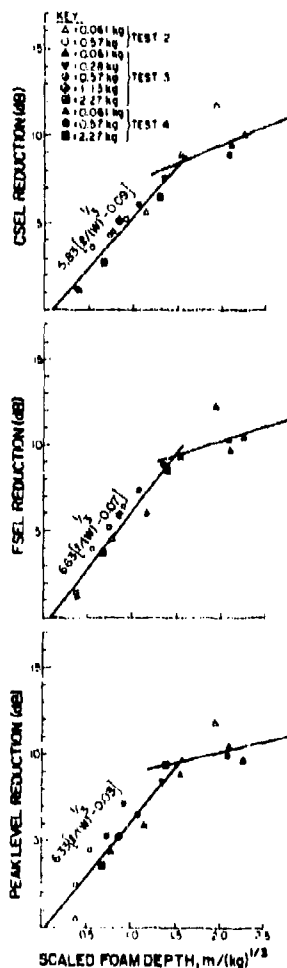


FIG. 3. CSEL, FSEL, and peak level reductions versus scaled foam depth: high expansion-ratio foam tests.

tions are uniformly about 12 dB. (In explosives work, it is common to use either energy or mass scaling to display data. In this case, the scaling used is the foam depth in meters divided by the cube root of the charge mass. This technique will be discussed further after the other tests are described.)¹

C. Test 3

Test 3 investigated the effect of charge size for a constant foam depth. The enclosure used in this experiment was 1.8 m on a side. Charge masses of 0.061, 0.28, 0.57, 1.13, and 2.27 kg were fired. These data are also displayed in Fig. 3 ($\nabla = 0.28$ kg, $\circ = 0.57$ kg, $\diamond = 1.13$ kg, $\square = 2.27$ kg). Because the wind knocked the foam depth down by 0.08 to 0.15 m before the explosive was fired, the geometric average of 1.7, 1.8, and 1.8 m was used in the data analysis. When the sound level reductions are plotted versus the cube root scaled foam depth, the plots increase linearly up to 1.2 m/kg^{1/3}; at larger scaled foam depths, the reductions appear to level off.

D. Test 4

When the data from tests 2 and 3 are plotted together, it is not clear which results correctly describe the behavior of the reduction at large scaled foam depths. The test 3 data show a clear break in the rate of reduction above 10 dB—the test 2 data do not. To investigate further, three experiments were performed.

(1) A 0.061-kg charge was detonated in a 1.6 × 1.6 × 1.5-m enclosure. Microphones were placed at 15 and 30 m—much closer to the charge than in tests 2 and 3—to determine if over land propagation differences could be the cause of the saturation and/or discrepancy in results.

(2) A 0.57-kg charge was centered and detonated in a 3.7 × 3.7 × 3.7-m enclosure with the microphones at 60 and 120 m.

(3) A 2.37-kg charge was centered and detonated in a 3.7 × 3.7 × 3.7-m enclosure with microphones at 60 and 120 m. Again, these results are shown in Fig. 3.

E. Discussion of tests 2-4

All data from tests 2-4 are plotted in Fig. 3 versus scaled foam depth. The foam depths used are the geometrically averaged foam depths or their equivalents. The lines shown are linear least squares fit to portions of the data. The first segment of the line is fitted to the data points from 0.0-1.6, the second segment from 1.2-2.5. From Fig. 3 it is apparent that:

(1) All the data obey the cube root scaling law, with the exception of the single data point from test 2, which lies well above the fitted line. This point is for a small charge mass, 0.061 kg, and such charges are generally unreliable. All of the other data points are within 1.5 dB of the lines.

(2) The maximum possible reduction is limited to about 10 dB. There appears to be a transition from a rapid increase in reduction under 1.2 scaled m to a much slower reduction over 1.2 scaled m. A similar saturation at 1.5 scaled m has been reported by Dady *et al.*⁴ in their investigation of the reduction of blast overpressures.

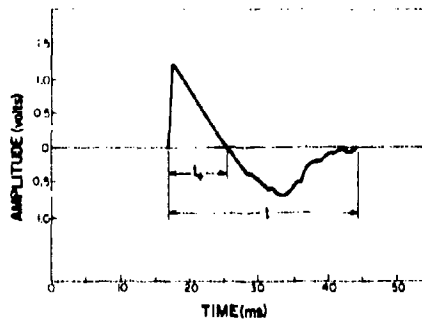


FIG. 4. Positive and total duration of a transient waveform typical of an explosion at close range.

(3) All metrics, CSEL, FSEL, and peak level, are reduced by roughly the same amount. The initial slopes are 5.8, 6.6, and 6.3 dB per scaled m, respectively. The small difference between the peak level slope and the FSEL slope indicates that the foam causes little duration change in the wave form, since the FSEL is a function of an integral over the duration of the wave.

To examine this more closely, the positive phase duration and total duration of the wave were monitored directly using a Bruel and Kjaer type 7502 Digital Event Recorder to display the transients on a screen. The positive and total durations were measured from this display (see Fig. 4). When plotted versus scaled foam depth, the positive phase duration was reduced by about 5% by the foam; the total duration was reduced by about 20%. Although there was great scatter, the total duration change tended to become smaller as the foam depth increased.

To check whether our farfield data agreed with past nearfield work, Winfield and Hill's data⁵ were scaled out to 60 m using a design chart of pressure versus distance.³ This technique is at best crude, since at close ranges energy is still being fed into the shock wave by the expanding detonation products, and the foam certainly must affect these energy transfers. This calculation also neglects the reflection of the shock wave at the foam/air interface. Still, the results of this calculation agree reasonably well with the data from our study. The initial slope of the peak pressure reduction versus scaled foam depth line is 8.6 vs 6.3 dB per scaled m measured in the present study. This difference may be due to the denser foam used by Winfield and Hill,⁵ or to the placement of their pressure transducers near the bottom of the foam volume, where the foam may be denser.

III. SERIES 2: LOW EXPANSION FOAM

A Mearl Corporation OT 10-5 generator was used for the dense foam experiments. The generator was adjusted to produce a stiff 30:1 expansion ratio foam at a reasonably high flow rate; the foam was made from a 5% solution of National Foam Systems 14% high expansion foam solution. The bubble diameter in this foam was on the order of a millimeter. The low expansion foam was quite stable; no drainage

or subsidence was noticeable in the first hour after generating the foam.

The experimental set up for the 30:1 foam tests was the same as that described for the high expansion foam. The knowledge gained from the high expansion foam results allowed a simpler experiment for the low expansion foam.

Three charge masses were used: 0.11, 0.57, and 2.37 kg. Three cubical enclosures were used with the 0.11-kg charge: 0.31, 0.91, and 1.5 m on a side. Five cubical enclosures were used with the 0.57-kg charge: 0.31, 0.61, 0.91, 1.2, and 1.5 m. Two cubical enclosure sizes were used with the 2.27-kg charge: 0.91 and 1.52 m. The enclosures were oversized by 0.2 m on length and width; thus, the foam depth used in the data analysis was the geometric average of the enclosure dimensions divided by two.

The reductions in noise level from the various trials and microphones were averaged. These are plotted in Fig. 5.

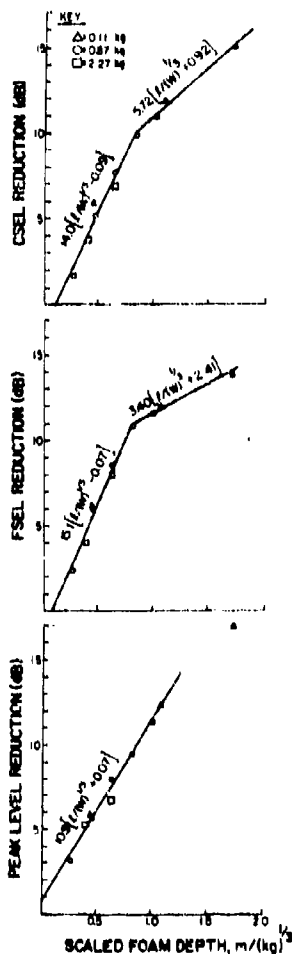


FIG. 5. CSEL, FSEL, and peak level reductions versus scaled foam depth; low expansion-ratio foam tests.

Three features in Fig. 5 are of interest.

(1) The data scale rather well; all the points lie close to the best fit lines when reduced to scaled coordinates. None of the points lie further from the fitted lines than 1.0 dB.

(2) As in the low expansion foam, the reduction in FSEL is not linear over the full range of scaled foam depth, but has a break point at about 0.80 scaled m. The first segment on the FSEL curve is fit to the points from 0.0-0.9 scaled m; the second segment is fit to the points from 0.8-1.3 scaled m. The CSEL has a similar break point near 0.82 scaled m. The peak level reduction does not display as clean a break point; however, the point corresponding to the largest scaled distance is under the curve fit to the rest of the points. In each case where present, the break point does occur at a 10-11-dB reduction—similar to the break points in the series 1 tests.

Above the break point, the rate of reductions in the low expansion ratio foam is greater than in the high expansion ratio foam.

(3) As with the high expansion foam, the low expansion foam reduced the FSEL more than it reduced the peak level. The initial slope of the peak level curve is about 11 dB per scaled m, while the initial slope of the FSEL curve is about 14 dB per scaled m. This again indicates that the foam slightly reduces the time duration of the waveforms.

To further investigate the characteristics of this reduction, positive and total durations were measured in several of the tests. Like the high expansion foam test data, the low expansion foam data displayed great variation in duration reductions. The dense foam reduced the positive duration by about 20%; the reduction in total duration was about 30%, with changes scattered down to 0% and up to 44%. Even for identical tests, the changes varied from 5%-30%. There is a small tendency for the duration change to get smaller as the foam depth increases, as in the case of high expansion foam. The 30% reduction in total duration corresponds to a 1.5-dB difference between peak and FSEL reduction, if no change in shape occurs.

IV. EFFECT OF FOAM DENSITY

Test series 1 and 2 considered only two different foam expansion ratios: 250:1 (high expansion ratio foam) and 30:1 (low expansion ratio foam). For each foam, a cube root scaled foam depth was used to organize the test results for widely varying charge sizes into a single set of curves for each sound level metric. The success in scaling the results for different charge masses in this way indicated that perhaps the two sets of data could be combined if plotted against a scaled variable which include the foam density. To pursue this possibility, the literature on blast scaling was examined.

An explosives scaling law which includes the density of the surrounding media is Lampson's earth shock scaling law⁶

$$(p_1 - p_0)/p_0 = h(\rho_0 R^3/w), \quad (2)$$

where

$h(\)$ is a function only of $\rho_0(R^3/w)$

ρ_0 is the density of the medium surrounding the charge

R is the distance from the charge center

w is the mass of the charge.

Since the reduction data from the tests of high and low expansion foams scaled well as a function of $(l^3/w)^{1/3}$, Lampson's scaling law suggests that plotting both sets of data as a function of $(\rho^3/w)^{1/3}$, where ρ is the foam density, may result in a unification of the predictions.

All of the data from test series 1 and 2, except for the data from test 1 of series 1, are plotted versus dimensionless foam depth in Fig. 6. The dimensionless foam depth used in this figure is the geometrically averaged foam depth multiplied by the cube root of the foam density in kilograms per cubic meter and divided by the cube root of the charge mass in kilograms of TNT. (When charge mass is used in scaling laws, it is common to express it in terms of an equivalent mass of TNT. The C-4 used in our experiments is about 1.34 times as energetic as TNT; to agree with scaling conventions, our charge masses were adjusted by that factor.) The dimensionless foam depth is

dimensionless foam depth is

$$X = (\rho^3/w)^{1/3}, \quad (3)$$

where

ρ is the foam density in kg/m^3

l is the geometrically averaged foam depth

w is the mass of explosive in kilograms of TNT.

The density of the foam is given by the density of water (1000 kg/m^3) divided by the expansion ratio.

From Fig. 6, we see that the data scale well for all metrics up to a dimensionless foam depth of 2.5. Little or no systematic differences were detected between the high and low expansion foam results. Thus the foam scaling laws and Fig. 6 can be used to predict the reduction produced by varying foam densities, foam depths, and charge masses. However, there are not enough data at different foam densities to establish that the foam scaling laws hold for widely varying foam densities. For example, in the extreme case of pure water (expansion ratio 1:1), the foam scaling laws do not hold. The reductions produced by water were measured by detonating a 0.57-kg charge of C-4 in the center of a 0.39-m cube. The dimensionless foam depth calculated for this experiment was 2.22, which by Fig. 6, would result in reductions of 8.0, 8.7, and 8.2 dB in CSEL and FSEL, and peak level, respectively. The actual average reductions, measured by microphones at 30, 60, and 120 m and averaged, were only 3.8, 3.7, and 5.7 dB.

The foam scaling laws do not hold for dimensionless foam depths greater than 2.5. Above 2.5, the denser foam produced greater reductions than the lighter foam.

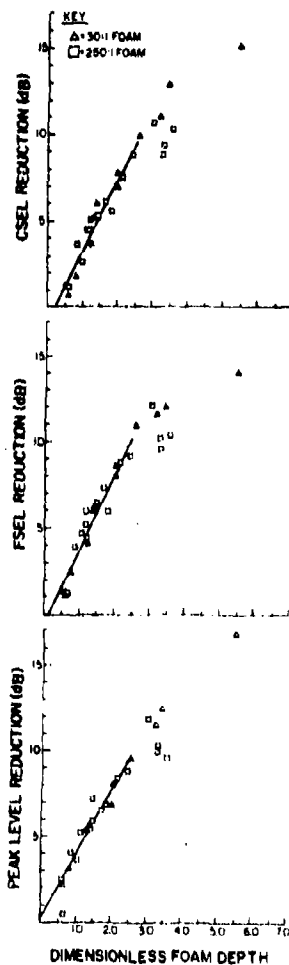


FIG. 5. CSEL, FSEL, and peak level reductions versus dimensionless foam depth.

V. DISCUSSION OF RESULTS

The results observed in these tests can be explained by a two mechanism model of blast noise reduction by foams. The noise reduction data clearly separates into two regimes, above and below a dimensionless foam depth of 2.5. Below 2.5, the data scales with density and displays a rapid reduction in noise level with increasing foam depth. Above 2.5 the rate of reduction is smaller and does not scale with density. The break point occurs at different scaled radii for the two foams, however, it occurs at about the same pressure. This pressure, calculated from the reduction data and the bare charge pressure³ is on the order of a few hundred kPa. From independent tests of foam collapse, it has been found that these pressures are very close to the minimum pressure necessary to fracture the foam cells and so form a fine water mist.⁷ With this knowledge it is evident that at least two distinct mechanisms of noise reduction are operative. (1) Strong wave decay through the water mist of the fractured foam; and (2) nonacoustic decay of the weak wave through the intact foam. The first mechanism is dominant close to the explosive, where peak pressures are very high; the second one dominates further out, in the low pressure regime.

In general, the decay of strong waves depends on the irreversible work performed on the fluid between its initial state (before the wave has arrived) and its final state (after the fluid has returned to ambient pressure).^{8,9} This is often called the waste or lost work and is related to the entropy produced

between the initial and final fluid states. For a homogeneous fluid, the source of lost work is viscous dissipation due to the very large strains across the thin wave front. In a two-component material like foam, however, other sources of irreversible work are also available; the slip and heat transfer between the air and water as the two components come to equilibrium are both irreversible processes. For high peak pressures, the water in the foam is broken into extremely fine droplets, each with a large specific surface area, so that the heat and momentum transfer between the two components is very rapid. This leads to substantial irreversible work in the small time available between the arrival of the front and passage of the wave. This may account for the observation that foams reduce sound levels more effectively than solid/air systems of comparable density. That is, solids cannot fracture into small particles that provide a very large surface area. In addition, the maximum possible strains are much larger in a foam than they are in air alone: the shock compression ratio in air is limited to about six; in dense foams, the rapid heat transfer from the air to the water permits a maximum compression ratio of about 30. Consequently, foams may exhibit enhanced strain-dependent entropy production.

Note that this intercomponent transport mechanism cannot be responsible for the observed reductions at large foam depths. At the small peak pressures in the foam at large depths, the particle velocity and temperature rise are so small that heat and momentum transfer between the air and water cannot generate significant irreversible work.

At large scaled foam depths, the peak pressures are very small. In this regime, a wave propagating in a homogeneous material would experience acoustic decay with (for spherical geometry) its characteristic inverse distance effect on the sound levels. Thus, if the foam were homogeneous, some finite scaled depth would provide the maximum attainable benefit available from a given foam. At larger scaled depths, the sound levels would decay at the same rate in air and in the foam and so no further reductions would be obtained; the data in such a case would break to form a horizontal line. Since the data show a continued small increase in reductions beyond the break point, we conclude that at large scaled foam depths the waves are experiencing a dispersive, slightly nonacoustic decay in the additional foam. A weak wave propagating through the foam is partially reflected at each interface. This partial reflection results in nonacoustic attenuation and dispersion of the wave.¹⁰ We will further examine the dispersion when we discuss the foam induced changes in the pulse duration.

We note that the combined scaling of Fig. 6 supports our two mechanism model. Below a dimensionless foam depth of 2.5 the data scale with density. Since the foam is shattered by the passing shock, the reduction depends only on density and not on details of foam dimensions or cell structure. We expect the scaling to hold in this range provided that the isothermal compressibility of the air/water mixture remains approximately that of air and that direct interaction between water particles (in the compressed state) is not significant.

We likewise expect that the density scaling law should

fail for large foam depths since our proposed farfield mechanism of low pressure weak decay depends not only on foam density but also on foam structure. The low expansion foam has a much smaller characteristic bubble size and so a much larger specific surface area than the high expansion foam. Therefore, it should cause a more rapid attenuation of the weak wave by reflections in the intact foam. This is observed in Fig. 5 where the attenuation rate above a dimensionless foam depth of 2.5 is much more rapid in the low expansion foam.

The duration changes measured for both foams also support our proposed two mechanism model. For the high expansion foams the positive duration was reduced by about 5% and the total duration by about 20%. The total reduction becomes smaller with increasing foam depths. For the low expansion foam, the positive duration was reduced by 20%, and the total duration reduced by 30%. Again, the total duration change becomes smaller with increasing depth. The large scatter in this data prevents a detailed analysis of these changes, but a consistent explanation can be given.

To understand the reductions in wave duration, we must address three influences: the duration of the wave delivered by the explosive, broadening of the wave as it travels through the foam (if present), and broadening as it propagates through the surrounding air to the microphones. For farfield measurements the last of these—growth of the positive-phase duration as the wave travels through the air—is dominant, provided that the peak pressure at the foam/air interface is not small.¹¹ Most of the positive duration is accrued in the air, so that even if the foam significantly altered the duration at the location of the interface, this would have only a small effect on the values measured at a large distance from the charge. The small reductions noted in the positive-phase duration are, therefore, probably due only to the lower peak pressures (when foam is used) and the consequent reduction in rate of growth of the pulse width in the air. As more foam is used, the wave broadening due to the dispersion inside the foam becomes significant enough to partially offset the diminishment due to reduced peak pressures, leading to an overall smaller reduction in the positive-phase duration.

Since the reductions in total duration are more pronounced than those for the positive phase, it is apparent that the foam must have a strong influence on the negative-phase duration. Because the negative duration is nearly independent of the length of travel of the wave and of the host material, this reduction (unlike that of the positive phase) must originate in a reduced total duration delivered by the explosive. This is attributable to the (visible) absence of afterburn observed for charges fired in the foam. Afterburn occurs when the detonation products are oxygen deficient. These products react with the surrounding air to produce about 20% of the total explosive energy of C-4. Afterburning is a relatively slow process and suppressing this reaction would substantially reduce the total duration. Although this mechanism reduces the total duration significantly, the overall energy reduction is small compared to the reduction produced by the other two mechanisms discussed above. A 20%

direct reduction in explosive energy corresponds to less than 1.0-dB reduction in the SEL and peak levels.

VI. CONCLUSION

Two densities of aqueous foam have been tested for use in reducing blast noise from a wide range of explosive masses. The low density 250:1 expansion-ratio foam gives an initial rate of reduction of 5.8, 6.6, and 6.3 dB per scaled meter of foam depth in the CSEL, FSEL, and peak level measurements, respectively. In each sound metric, a break occurs in the reductions at about 10 dB; this takes place at a scaled foam depth of $1.5 \text{ m/kg}^{1/3}$ and additional foam beyond this point gives a much smaller rate of noise reduction.

The high density 30:1 expansion-ratio foam produces initial rates of reduction of 14.0, 15.1, and 10.9 dB per scaled meter of foam depth in the CSEL, FSEL, and peak sound levels. As with the low density foam a break occurs in the rate of reduction of the FSEL and CSEL at a 10-dB total reduction. In the high density case, however, the break takes place at a smaller scaled depth of about $0.9 \text{ m/kg}^{1/3}$. No clear break in the rate of reduction of the peak level was found for the high density foam.

When all the test data are scaled by the foam density as well as the explosive mass, the reduction results for both the high and low density foams fall on a single curve for each sound metric—up to a dimensionless foam depth of 2.5. Below this dimensionless foam depth, our proposed mechanism of noise reduction is the strong-wave decay due to irreversible intercomponent heat and momentum transfer between the air and water in the foam. This mechanism depends only on the density and not details of the foam structure.

Above a dimensionless foam depth of 2.5 the high den-

sity foam gives a larger rate of reduction than the low density foam. In this regime, the apparent mechanism of mitigation is the reflection of the waves within the intact foam. The high density foam gives a larger rate of reduction here only because of its smaller cells and larger internal surface area. The rates of reduction in the sound metrics is much smaller in both foams above a foam depth of 2.5, indicating that the strong-wave mechanism is significantly more important than the nonacoustic decay mechanism for noise reduction.

¹Assessment of Community Response to High Energy Impulsive Sounds, Working Group 84 of the National Research Council, (National Academy P., Washington, DC, 1981).

²Army Regulation 200-1, *Environmental Protection and Enhancement* (Department of the Army, June 15, 1982), Chap. 7.

³W. E. Baker, *Explosions in Air* (Univ. Texas, Austin, 1973).

⁴D. A. Dudley, E. A. Robinson, and V. C. Pickett, "The Use of Foam to Muffle Blast from Explosions," paper presented at the IBP-ABCA-5 meeting (June 1976).

⁵F. H. Winfield and D. A. Hill, "Preliminary Results on the Physical Properties of Aqueous Foams and their Blast Attenuating Characteristics," Tech. Note No. 389 (Defense Research Establishment, Alberta, Canada, Aug. 1977).

⁶U. Ericsson and K. Eden, "On Complete Blast Scaling," *Phys. Fluids* 3, 892-895 (1960).

⁷A. A. Ranger and J. A. Nicholls, "Aerodynamic Shattering of Liquid Drops," *AIAA J.* 7, 285-290 (1969).

⁸A. A. Borisov, B. E. Gel'fano, V. M. Kudinov, B. I. Palamarchuk, V. V. Stepanov, E. I. Timofeev, and S. V. Khomik, "Shock Waves in Water Foams," *Acta Astronaut.* 5 1027-1033 (1978).

⁹T. H. Pierce, "Blast Wave Propagation in a Spray," *J. Fluid Mech.* 88 (4), 641-657 (1977).

¹⁰J. S. de Krasinski, A. Khosla, and V. Ramesh, "Dispersion of Shock Waves in Liquid Foams of High Dryness Fraction," *Arch. Mech.* 30, 461-475 (1978).

¹¹D. T. Blackstock, "Nonlinear Acoustics (Theoretical)," *Amer. Inst. Phys. Handbook*, edited by D. E. Gray (McGraw-Hill, New York, 1972), Chap. 3n.

ATTENUATION OF BLAST WAVES WHEN DETONATING EXPLOSIVES INSIDE BARRIERS

JOSEPH M. POWERS and HERMAN KRIER

*Dept. of Mechanical & Industrial Engineering, University of Illinois, Urbana, IL 61801
(U.S.A.)*

(Received February 19, 1985; accepted in revised form August 22, 1985)

Summary

Noise produced by blast waves can be a problem, especially when an explosion occurs near populated areas. As one means of reducing the blast noise, the explosive is detonated in a pit, a space closed at the bottom and sides, open at the top. A two-dimensional finite difference model was used to simulate such an explosion in a pit and to determine to what extent the blast wave was attenuated. The code used, CSQ, developed by scientists at Sandia National Laboratories, was tailored for our studies. The key results were: (a) the presence of a pit in all cases caused the blast wave to be attenuated; (b) for a cylindrical pit, a pit of a radius which effected maximum blast wave attenuation was found; (c) a useful parameter, dE_{out}/dt , the energy loss rate from the pit, was shown to be a good indicator of relative pit effectiveness.

Introduction

It is possible to reduce the noise and the possible blast damage resulting from an explosive reaction by placing the explosive material in a partially open, thick-walled container or, in other words, in a pit. Examples of applications would include finding ways to reduce the blast noise near blasting sites used by geologists to find underground oil and gas, and determining appropriate ways to dispose of explosive armaments near populated areas.

Questions that need to be answered to determine ways to utilize pits surrounding an explosive to mitigate blast effects include the following:

- (1) What is the optimum horizontal distance from the charge to the pit walls in order to minimize the leading edge pressure at a fixed observer location?
- (2) What is the minimum vertical distance (floor to open top) to effectively reduce the blast noise at a fixed observer distance from the pit?
- (3) What parameters (other than the peak pressure pulse measured at an observer location) can be calculated to design the most effective pit?
- (4) What is the effect of energy-absorbing pit walls?

In this study we modelled the dynamic processes in and surrounding the pit by providing the solution to the time-dependent equations which conserve mass, momentum, and energy of the gases produced by the explosive as well as the air inside the pit. Clearly, a minimum of two independent space dimensions is required. The blast produces shocks and strong compression waves which propagate at supersonic speeds relative to the undisturbed air. The waves can move several kilometers per second. A km/s is also one mm/ μ s, and therefore it follows that the flow variables pressure, density, and energy need to be calculated at microsecond (10^{-6} s) time levels since changes in the flow variables occur over distances in the scale of millimeters or less.

The code CSQ, developed by scientists at Sandia National Laboratories, documented in a Sandia Technical Report [1], was used to model the problem.

Governing equations

The two-dimensional, time-dependent, Lagrangian form of the governing equations of conservation of mass, momentum, and energy in cylindrical coordinates used are

Conservation of mass

$$\frac{\partial \rho}{\partial t} = -\rho \left[\frac{1}{r} \frac{\partial (rv_r)}{\partial r} + \frac{\partial v_z}{\partial z} \right] \quad (2.1)$$

Conservation of momenta

$$r: \rho \frac{\partial v_r}{\partial t} = \frac{-\partial}{\partial r} (\sigma_{rr} + Q_{rr}) - \frac{\partial \sigma_{rz}}{\partial z} - \frac{\sigma_{rr} - \sigma_{\theta\theta}}{r} \quad (2.2a)$$

$$z: \rho \frac{\partial v_z}{\partial t} = \frac{-\partial}{\partial z} (\sigma_{zz} + Q_{zz}) - \frac{\partial \sigma_{rz}}{\partial r} - \frac{\sigma_{rz}}{r} \quad (2.2b)$$

Conservation of energy

$$\frac{\partial E}{\partial t} = - (P + \tilde{Q}) \frac{\partial}{\partial t} \left(\frac{1}{\rho} \right) \quad (2.3)$$

Here ρ represents density; t , time; r , the radial coordinate; v_r , the particle velocity in the x direction; z , the height coordinate; v_z , the particle velocity in the z direction; $\partial/\partial r$ and $\partial/\partial z$, the partial derivatives with respect to the Lagrangian coordinates, r and z , respectively; $\partial/\partial t$, the partial derivative with respect to time; σ , the stress tensor; Q , the artificial viscosity; P , the material pressure; and E , the specific material energy. These equations must be supplemented with an equation of state to have a determinate system.

Application of CSQ to the explosion-in-pit problem

As stated earlier, the program CSQ has been used to model the detonation of a high explosive surrounded by air in a cylindrical pit open to the atmosphere. Figure 1, the half-section view of a right circular cylinder, shows the features and gridding of a typical configuration. By placing the explosives at the center of the pit, it is possible to reduce the problem from three dimensions to two, with symmetry in the angular (θ) direction.

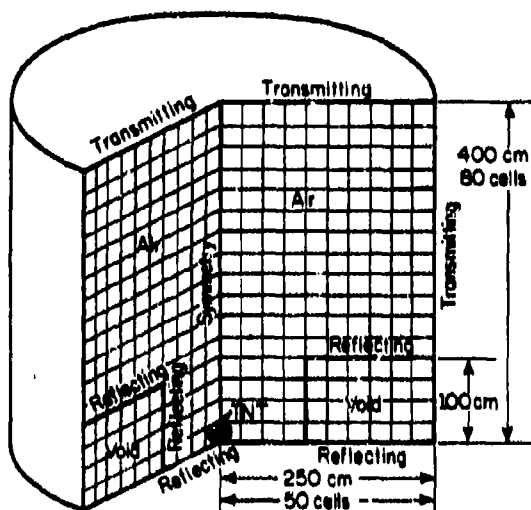


Fig. 1. Descriptions of the grid used by CSQ to model cases of varying charge mass, ambient temperature, and pit radius.

Two types of boundary conditions were employed, reflecting and transmitting. In all cases considered in this study, pit walls were treated as perfectly reflecting boundaries. Velocities at reflecting boundaries were defined to be zero. At transmitting boundaries, mass, momentum, and energy fluxes were permitted. CSQ used appropriate extrapolation schemes to determine the magnitudes of the fluxes.

CSQ is a two-dimensional (planar or cylindrical) hydrodynamic, Lagrangian code which is capable of solving many problems given an equation of state for each material and proper initial and boundary conditions. Given a configuration, CSQ will use finite difference techniques to advance the system in time. Details of the differencing scheme employed by CSQ are found on pp. 78-87 of Ref. [1]. Acceleration, velocity, position, density, and cell volume of each Lagrangian cell are determined using explicit finite difference relations. The energy equation and equation of state are then solved simultaneously using what is essentially a Newton-Raphson technique. At this point all thermodynamic quantities are known.

In order to run CSQ, the user must define the problem. This is accomplished by executing the program CSQGEN, in which the geometry, gridding, flow variables, thermodynamic properties and equation of state information for each material are defined. The finite difference grid is fixed. It is allowed to move during Lagrangian calculations but is then rezoned back to its original position. This rezone gives the code an Eulerian nature.

CSQGEN also requires equation of state information for each material. In the case studied, this meant providing tabular data for air and appropriate constants for the JWL [2] form of the equation of state for the explosive, TNT. Two thermodynamic properties of each material must be defined as an initial condition in CSQGEN along with the velocity of each material.

The tabular data for air were provided by Sandia National Laboratories. The data describe the nonideal nature of air at high temperatures. Data were available for temperatures ranging from 232 K to 2.82×10^6 K and for densities ranging from 1×10^{-9} g/cm³ to 3×10^{-2} g/cm³. This yielded data for a range of pressures from 1.0 dyne/cm² to 1×10^{12} dyne/cm². For all problems studied, the properties of the air remained within these limits.

Among the many quantities that were varied in the system studied were pit geometry, charge mass, and ambient temperature of the surrounding gas [3]. However, each problem studied retained certain basic features, namely,

- (1) A spherical charge of a high explosive sharing a common centerline with a right circular cylinder, lying on the base of the cylinder was detonated,
- (2) Interactions occurred when the spherical wave generated by the explosion struck a reflecting boundary, and
- (3) Fluid motion occurred outside the pit.

Detonation

The detonation of a high explosive is characterized by the progression of a detonation wave which moves at a constant velocity, D , and which leaves the reacted material at a pressure, P_{Cj} , the Chapman-Jouguet pressure. The variables D and P_{Cj} are specific to the explosive and are, in general, calculable quantities. Details on this are well-documented [4] and will not be repeated here. The propagation of the detonation wave through the high explosive was modelled. The behavior of a spherical blast wave which is surrounded only by air is well-known. The problem is one-dimensional in the radial direction in spherical coordinates. Relations which predict pressure as a function of radius are given, for example, by Baker [5].

CSQ was used to simulate the unconfined explosion of a spherical charge of TNT, $r = 1$ cm, in air at standard atmospheric conditions. Since the code is a finite difference code in cylindrical coordinates, a true sphere cannot be defined. The spherical charge is simulated by a set of cylindrical finite difference cells. Cells of mixed composition are allowed, so it was possible to have the mass of explosive which corresponded to the specified charge

radius and density. Cells of mixed composition were treated as a homogeneous mixture; no internal boundaries existed.

Results of this calculation are shown in Fig. 2, along with three results obtained by other means. The peak pressure at a given distance from the charge center is plotted as a function of the number of charge radii away from the charge center. CSQ's predictions were arbitrarily made along the vertical centerline. Two of the other predictions shown, found in Baker's book [5], are based on experiments. The other predictions shown, made by Griffiths [8], is based on calculations that assumed a radially one-dimensional pressure wave. It is seen that none of the four methods agree perfectly, but that CSQ predicts pressures in the same range as those predicted by the one-dimensional methods.

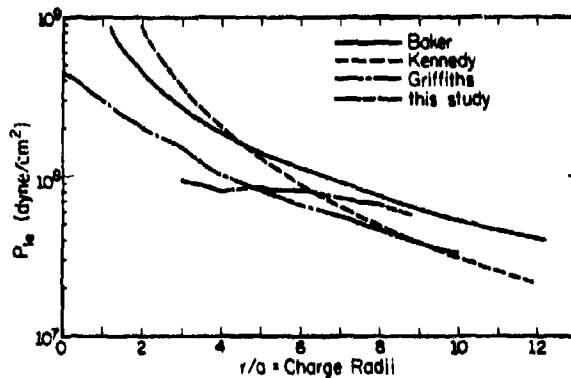


Fig. 2. Predictions for the pressure at the leading edge of the radially one-dimensional spherical blast wave by various methods.

Interaction of waves with boundaries

As stated earlier, complex interactions between spherical shock waves and reflecting surfaces, both planar and cylindrical, occurred in the problem modelled. In Ref. [3] the CSQ code was used to model a simple case of a shock wave interacting with a reflecting boundary. The problem modelled was the classical one-dimensional, linear shock tube, divided into two regions, one of high pressure air and the other of low pressure air. The system was assumed to be in thermal equilibrium. The results obtained from the solution of the analytic equations given by Shapiro [7] and the results from the application of CSQ were almost identical for the pressure behind the initial shock and the pressure behind the shock reflected from the closed end. Since the linear, one-dimensional reflections were accurately modelled, it was assumed that CSQ could accurately predict more complicated reflections such as those that result when explosions occur in pits.

Complicated two-dimensional wave interactions were modelled. The wave motion is easily described in the early stages by a simple spherical blast wave. Upon striking the cylindrical wall, a shock wave is reflected towards the pit center. This shock interacts with the initial blast wave. Soon after this, all combinations of interactions (shock-shock, shock-expansion, shock-wall, etc.) are possible. An accurate verbal description becomes nearly impossible.

Two limiting cases can be easily described. With R as the radius of the pit and H as its height, the parameter R/H is a characteristic of the pit. As R/H approaches infinity, an explosion in the pit behaves essentially as if there were no pit; it is really an unconfined explosion except for the interaction with the horizontal surface, which only serves to double the effective charge energy. At the other end, as R/H approaches zero, the blast wave attains a linear nature. Reflections occur, and the resulting wave looks like a planar wave propagating through a tube.

As the blast wave leaves the pit, it begins to behave spherically. Behind the initial front, waves are still interacting, and they too leave the pit. In some cases studied it was observed that these waves catch up to and strengthen the initial blast wave. A feature noticed in all cases was a vortex which developed on the surface outside the pit near the pit wall.

A final feature of problems studied is the relatively long computation time required to model the problem. In most cases the maximum number of cells was used in order to achieve the most accurate results. As more cells are used, computation time to model equivalent systems increases. To model the detonation of a charge of TNT required about 1000 CP seconds on the University of Illinois's CYBER 175 computer. Once this foundation was built, tests varying pit geometry could be made.

Results

Numerical tests were conducted which predicted the history of the cumulative amount of energy which had left the pit. Other numerical tests examined the flow-field both in and outside of the pit. The parameters which were varied were (a) pit height, (b) pit radius, (c) charge mass, and (d) ambient temperature.

For this study, we define an effective pit on a relative scale. For the general problem of the detonation of high explosives within a partially enclosed volume, one can state that the more the pressure wave that results from the detonation is attenuated, the more effective is the partially enclosed volume. As stated before, the partially enclosed volumes studied were cylindrical volumes which were closed at the base, closed at the sides, and open at the top; or, more compactly, pits. The tests were limited to models of explosions of spherical charges of TNT lying on the bottom of the cylindrical volume at its centerline.

Flow-field inside pit: E_{out} versus time

As one means of determining pit effectiveness, the time derivative dE_{out}/dt is calculated. E_{out} is the cumulative amount of energy, both internal and kinetic, which has left the pit. This number results from the utilization of the transmitting boundary condition defined to exist at the top of the mesh. The transmitting boundary condition allows fluxes in and out of the mesh by defining flow variables outside of the mesh to be extrapolated values of the flow variables in the mesh.

We believe that as pit effectiveness increases, energy release decreases, causing the downstream pressure pulse to be weaker. A less effective pit would allow a rapid release, causing the pressure pulse to more closely resemble the pressure pulse that would exist had no pit been present. The measure of pit effectiveness dE_{out}/dt is a qualitative measure. It is useful for cases in which a single parameter is varied.

E_{out} versus time for explosions in pits

Three pit heights were modelled in these tests. Pit radius was maintained at 100 cm. A charge of TNT, $r = 1$ cm (mass = 6.83 g), was used in all cases, and ambient conditions of the surrounding air were taken as standard atmospheric. The three pit heights modelled were 0.4, 1.2, and 2.0 m. To eliminate any possible grid biasing between the three cases, a constant cell size was used, namely 5.714 cm by 2.857 cm. This resulted in variable grid dimension for each case, 35×35 for the 2.0 m height, 21×35 for 1.2 m, and 7×35 for 0.4 m.

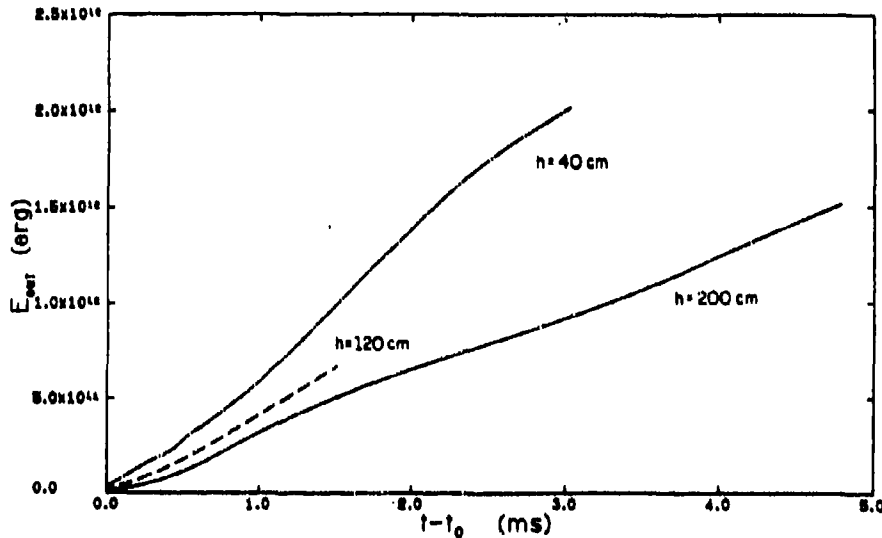


Fig. 3. CSQ prediction of E_{out} versus time for detonations in cylindrical pits of variable height.

The predictions for E_{out} are shown in Fig. 3. Here, E_{out} is plotted as a function of $(t - t_0)$, where t_0 is the time when energy was first predicted to escape the pit.

As the results clearly indicate, dE_{out}/dt increases as pit height decreases. For any given time, more energy will have left the shorter pit than the taller pit. From this we conclude that if a blast wave is partially enclosed by a cylindrical pit with reflecting walls, as the wall height increases, the blast wave appears to have been produced by a charge of smaller mass. In summary, as pit height increases, dE_{out}/dt decreases, and pit effectiveness increases.

Flow-field outside pit: P_{le} versus r

In order to obtain qualitative results, namely, the flow-field variables outside the pit, it was decided to expand the domain of the problem to include the volume outside the pit. In all further tests, a constant grid geometry, shown earlier in Fig. 1, was maintained. The number of cells used, 4000, corresponding to a 50×80 grid, is close to the maximum number available in our CYBER 175 computer.

Variable pit radius

A series of tests was performed that modelled the detonation of a sphere of TNT, $r = 1$ cm, surrounded by air at standard atmospheric conditions. The charge was located at the bottom center of a cylindrical pit of constant height, 100 cm, and variable radius. Six cases were modelled, with the pit radii in the tests being 20, 25, 35, 50, 75, and 150 cm. The geometry of the configuration is seen in Fig. 4.

Figure 5 shows some pressure—distance results of these tests. Here the predicted pressure of the leading edge of the wave at points on the horizontal surface outside the pit is plotted as a function of distance from the bottom center of the pit for pits of various radii. Also shown are results for $r = \text{infinity}$, which corresponds to the case where no pit is present; only the horizontal surface exists. Far from the charge, this case is equivalent to the unconfined explosion of a charge of twice the original charge's mass.

By the previous definition of an effective pit, we say that at a given distance from the charge, the lower the pressure, the more effective the pit.

Some key features illustrated on this figure are:

- (1) the decay of the leading edge pressure with increasing distance from the charge center is predicted in all cases studied,
- (2) at all points on the horizontal surface outside the pit, the existence of vertical barrier walls is predicted to make the pit more effective than a pit with no barrier walls, and
- (3) the existence of a minimum leading edge pressure as a function of pit radius is predicted. That is, it is predicted that at a given distance R from the charge center, the derivative $\partial P_{le}/\partial r_{pit}$ is zero when evaluated at

a certain barrier radius, and this critical point is a point of minimum pressure.

The existence of the minimum is seen more clearly in Fig. 6 in which the pressure at the leading edge of the wave at two points along the horizontal surface (outside the pit) is plotted as a function of pit radius. At this distance, the most effective pit has a radius of approximately 50 cm.

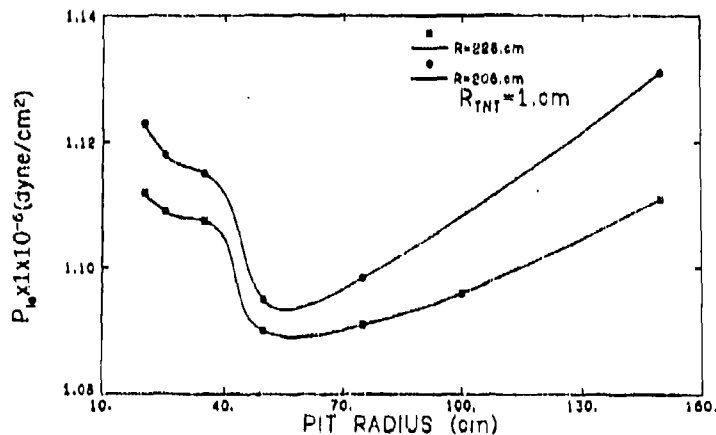


Fig. 6. Predicted pressure at leading edge at a point on the surface outside the pit versus barrier radius.

Point 3 deserves some amplification and speculation. First, the existence of this minimum was not expected. What was expected was that pit effectiveness would increase as pit radius decreased. A pit of infinite radius is really no pit at all; it is an unconfined region. As the radius is brought in from infinity to zero, it was expected that the pit would have more and more of a damping effect on the blast wave. The increased damping effect was predicted by CSQ, but only to a point at which other factors must have influenced the flow's behavior.

One possible explanation is that the original expectations are indeed true in the far-field. Possibly the domain of the problem studied is not large enough to observe this, and therefore it may be true that only a near-field phenomenon has been observed.

Another possible explanation of the minimum is related to secondary waves trailing the leading edge wave. In all cases, CSQ describes secondary waves reflected from the various surfaces in the domain. It is noted in some cases that these secondary waves leave the fluid at a higher pressure than the leading edge wave did at the same point. As pit radius shrinks, it is predicted that the secondary waves overtake and strengthen the leading edge wave. This presents the possibility that in the far-field, all secondary waves will eventually strengthen the leading edge wave, possibly rendering any attenua-

tion by the pit to be nonexistent. This is plausible for the system studied, since the reflecting walls do not remove any energy from the blast wave.

Regardless of why the minimum is observed, a consequence of its existence is important. Because of the minimum, if one were designing a pit to attenuate a blast wave, an optimum pit radius could be determined.

Variable charge mass

Simulations testing the effect of charge mass were carried out. In these tests, the detonation of a spherical charge of TNT, $r = 8$ cm (mass = 3497 g), rather than $r = 1$ cm, was modelled. Again, the charge was surrounded by standard atmospheric air and a pit of constant height, $h = 100$ cm, and variable radius, $r = 20, 25, 35, 50, 100, 150$ cm.

Figure 7, similar to Fig. 5, shows the predicted pressure at the leading edge of the wave at points along the horizontal surface outside the pit as a function of distance from the bottom center of the pit for pits of various radii, including infinite radius. The same features noticed in the earlier series of tests (with a smaller explosive charge), decay of the leading edge pressure with distance from charge center, the ability of the pit to attenuate the blast wave, and the existence of a barrier radius which yields a minimum leading edge pressure, are all predicted here. However, at these higher blast pressures one notices that predicted behavior is less explainable. The pressure-distance results exhibit different features than the results obtained for the explosion of the smaller, $r = 1$ cm charge. For example, a point of maximum pressure at a given barrier radius is predicted for $r_{\text{pit}} < 35$ cm. The only explanation offered for this is that stronger shock waves tend to make systems less linear, and thus, generally much more difficult to describe.

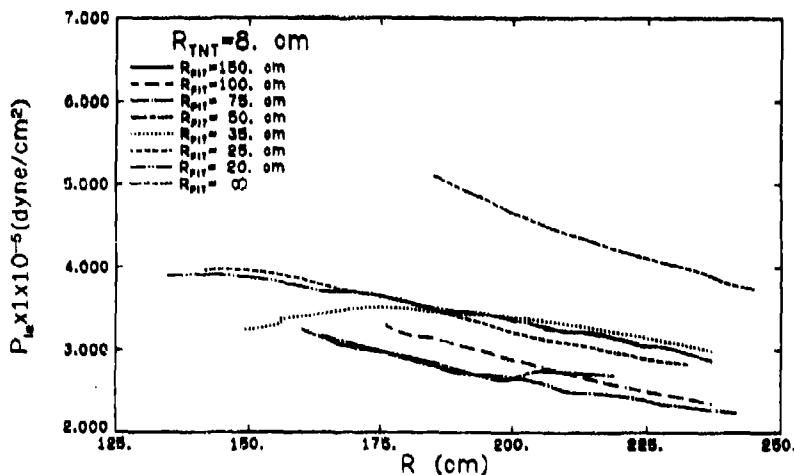


Fig. 7. Predicted pressure on surface outside of pit of the leading edge versus distance from the bottom center of the pit for pits of variable radius.

Variable ambient temperature

Another test conducted varied the ambient temperature of the surrounding air. Three cases were studied, one with the temperature of a cold day, 245 K (-18.4°F), one at standard atmospheric conditions, 298 K (77.0°F), and one with the temperature of a hot day, 320 K (116.6°F). In all cases, the pressure was maintained at standard atmospheric level and the density adjusted to satisfy the equation of state for air. The detonation of a charge of TNT, $r = 1$ cm, lying at the bottom center of a pit radius 25 cm, height 100 cm is modelled. In all three cases, it was seen that ambient temperature had no effect on the pressure at the leading edge of the wave in the domain studied.

Conclusions and Recommendations

The main conclusions that can be drawn from the results of this study are:

- (1) By using the two-dimensional, axisymmetric finite difference form of the governing equations of conservation of mass, momentum, and energy, along with equations of state for the materials studied, it is possible to model explosions and describe interactions between highly nonlinear shock waves and reflecting boundaries.
- (2) When a high explosive of fixed mass at the bottom of a pit is detonated, the resulting pressure wave has less strength outside the pit than that which would have existed had the blast not been contained by the pit. This was clearly shown in Fig. 5, where one can see that at any given distance from the source of the explosion, the pressure at the leading edge of the blast wave for contained explosions is less than the leading edge pressure for an uncontained explosion.
- (3) For explosions in pits of variable radius and constant height, there exists a pit radius which will minimize the pressure at a given distance from the charge center. Figure 6 displayed the leading edge pressure versus pit radius at two constant distances from the charge center. It was clearly demonstrated that a minimum pressure does exist, which implies that there is a pit geometry for maximum effectiveness.

It is clear that we should look for experimental data which could be compared with our results prior to attempting complicated and time-consuming refinements to the studies carried out. Lacking such data, some modifications could be made.

An important improvement to our study would be to introduce absorbing walls, rather than to continue to use totally reflecting walls. This would have several ramifications. First, the model would be more realistic. In the actual process of shock reflection, perfect reflectors do not exist. Accurate modeling of walls which absorbed a portion of the shock wave's incident energy could only improve the calculated results. Secondly, absorbing walls would most likely attenuate the blast wave in the air. This is a simple application of the principle of conservation of energy. A portion of the blast wave's energy

would go into the irreversible compression of the absorbing wall. This loss of energy would weaken the blast wave, and thus increase pit effectiveness.

It should be noted that an appropriate boundary condition for the interface where the solid wall material contacts the outer edge of the domain would have to be determined. No such condition would be necessary at interior interfaces of wall material and gas; interior interfaces are handled internally by CSQ.

Finally, it should be noted that viscous effects in the gases were assumed to be negligible. As the wave progresses into the far-field, viscous attenuation and vibrational relaxation become the more dominant mechanisms for weakening the wave [8]. It may be profitable to examine these effects at a later date.

Acknowledgements

We acknowledge the assistance given by Dr. Barry Butler, now at the University of Iowa, in both the theoretical and the programming segments of the study. Also for their help in getting the program CSQ to execute, we thank Drs. Tom Bergstresser and Bill Davey of Sandia National Laboratories. The insights of Drs. Stewart Griffiths of Sandia and Richard Raspet of CERN, Champaign, Illinois, were also valuable. The work was funded by U.S. Army, Construction Engineering Research Laboratory, Champaign, Illinois. Dr. Richard Raspet was Program Manager.

References

- 1 S.L. Thompson, CSQII - An Eulerian finite difference program for two-dimensional material response - Part 1. Material Sections, SAND77-1339, Sandia National Laboratories, Albuquerque, NM, 1979.
- 2 J.W. Kury et al., Metal acceleration by chemical explosives, in: Fourth Symposium (International) on Detonation, U.S. Government Printing Office, Washington, DC, 1965, pp. 3-13.
- 3 J.M. Powers and H. Krier, Blast wave attenuation by cylindrical reflecting barriers: A computational study, University of Illinois Report, UILU ENG-84-4014, 1984.
- 4 W. Fickett and W.C. Davis, Detonation, University of California Press, Berkeley, CA, 1979.
- 5 W.E. Baker, Explosions in Air, University of Texas Press, Austin, TX, 1973.
- 6 S. Griffiths, Aqueous foam blast attenuation, Internal Report, Sandia National Laboratories, Albuquerque, NM, Private Communication to Professor H. Krier and Dr. R. Raspet, September 1982.
- 7 A.H. Shapiro, The Dynamics and Thermodynamics of Compressible Flow, Vol. II, The Ronald Press Company, New York, NY, 1954.
- 8 H.E. Bass, J. Ezell and R. Raspet, Effect of vibrational relaxation on rise times of shock waves in the atmosphere, Acoust. Soc. Amer., 74 (5) (1983).

SHOCK PROPAGATION AND BLAST ATTENUATION THROUGH AQUEOUS FOAMS*

TIMOTHY D. PANCZAK, HERMAN KRIER

Department of Mechanical and Industrial Engineering, University of Illinois, Urbana, IL 61801 (U.S.A.)

and P. BARRY BUTLER

Department of Mechanical Engineering, University of Iowa, Iowa City, IA 52242 (U.S.A.)

(Received November 5, 1985; accepted in revised form August 22, 1986)

Summary

Experiments cited in this paper reveal that aqueous foams are good attenuators of blast waves and the resulting noise. A model is presented which describes the behavior of an explosively produced blast wave propagating through aqueous foam. The equation of state for an air/water mixture is developed with specific attention to details of liquid water compressibility. Solutions of the conservation equations in a spherically one-dimensional form were performed using a finite-difference wave propagation code. Results are presented that indicate the effect of the foam expansion ratio as well as the dimensionless foam depth on the blast attenuation. The (limited) comparison of decibel level attenuation between the model and the experiments shows good agreement.

Introduction

Spherically symmetric blast waves resulting from explosions in air can cause serious damage to structures located many charge radii from the center. In addition, the blasts also produce significant levels of environmental noise at distances beyond the region of structural damage. Consequently, the areas where blast-producing activities (such as demolition work and ordnance disposal) can be conducted safely are limited.

When a detonation wave propagating through a condensed explosive reaches the air/explosive interface, an intense shock wave with pressures of the order of hundreds of atmospheres is propagated radially outward through the air. It has been shown [1] that the strength of the blast wave can be greatly attenuated by surrounding the explosive charge with aqueous foam. An aqueous

*Work supported by U.S. Army, Construction Engineering Research Laboratory, Champaign, IL; Dr. Richard Raspet was Program Monitor.

foam consists of a matrix of thin sheets of water encapsulating tiny pockets of air. By adding a surfactant to the water to increase the surface tension, foam can be produced in a wide variety of expansion ratios. These foams are most commonly produced by commercial fire-fighting equipment. The expansion ratio is defined as the ratio of foam volume to liquid volume

$$\alpha = v_f/v_l \quad (1)$$

Raspet and Griffiths [1] summarize past experimental work on shock attenuation and include extensive data on far field attenuation of peak pressure, flat weighted integrated sound exposure levels (FSEL) and C-weighted exposure levels (CSEL) for a variety of charge masses, foam depths and foam expansion ratios. Also presented are scaling laws which relate the foam depth, foam density and charge mass to the noise reduction levels.

Figures 1a-c show reduction levels for various depths of 30:1 expansion ratio foam [1]. In these figures the foam depth is scaled to the cube root of the charge mass. The experiments were conducted using three different charge masses, 0.11 kg, 0.57 kg and 2.27 kg. The reductions are plotted in dBs (decibels) with the peak pressure level defined as $20 \log (P_{\max}/P_o)$ where P_{\max} is the maximum pressure and P_o is a reference pressure, $P_o = 20 \mu\text{Pa}$. The sound exposure level (SEL) is defined as

$$\text{SEL} = 10 \log \frac{\int P^2 dt}{P_o^2 t_o} \quad (2)$$

where t_o is a reference time defined to be one second. The integral in eqn. (2) is performed over the entire duration of the wave form, both positive and negative phase. The FSEL is calculated with no frequency weighting and the CSEL is calculated with a standard C-weighting filter. In all configurations, two trials were performed and FSEL, CSEL and peak pressure were measured at both 60 m and 120 m from the charge center. Figures 2a-c show the 30:1 data combined with data for a much less dense 250:1 foam. Here, the authors included foam density ρ_f in the scaled depth. In Figs. 2a-c the dimensionless foam depth is defined as

$$X = \Delta r [\rho_f/M]^{1/3} \quad (3)$$

where ρ_f is the foam density [kg/m^3], Δr is the geometrically averaged foam depth [m], and M is the mass of the explosive [kg] (TNT equivalent).

In addition to peak pressure and sound exposure level reduction, Ref. [1] also notes a decrease in both the total and positive phase durations of the far field recorded wave form when foam is the wave propagation medium. Plotted as a function of scaled foam depth these dB reductions were 20% and 5%, respectively. As shown in Fig. 1, the maximum reductions in CSEL, FSEL and peak pressure were limited to about 10 dB.

An interesting result presented in Ref. [1] is that the attenuation is shown

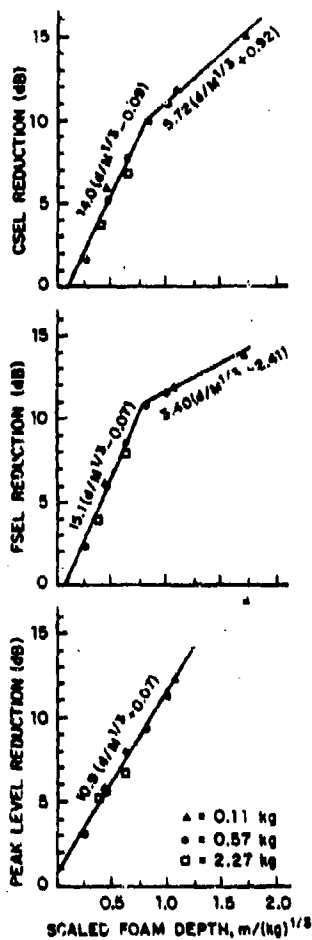


Fig. 1. Reductions for $\alpha = 30$ foam (from Ref. [1]). The scaled foam depth is defined as the ratio of foam depth d to the cube root of charge mass M .

to be linear with scaled foam depth up to a certain nondimensional depth (0.8 for 30:1, 1.5 for 250:1). For depths greater than this the foam still shows increasing attenuation with depth but at a much less effective rate. A two-mechanism model was proposed [1] to explain this bilinear behavior. First, it was assumed that in the near-field the shock pressure is strong enough to break the foam structure into microdroplets across the compressive shear layer of the shock front. This insures an extremely quick equilibration of velocity and temperature between the two phases and allows one to consider the air/water foam system as a homogeneous material. Second, when the shock is no longer strong enough to shatter the foam structure, it is assumed that the air and

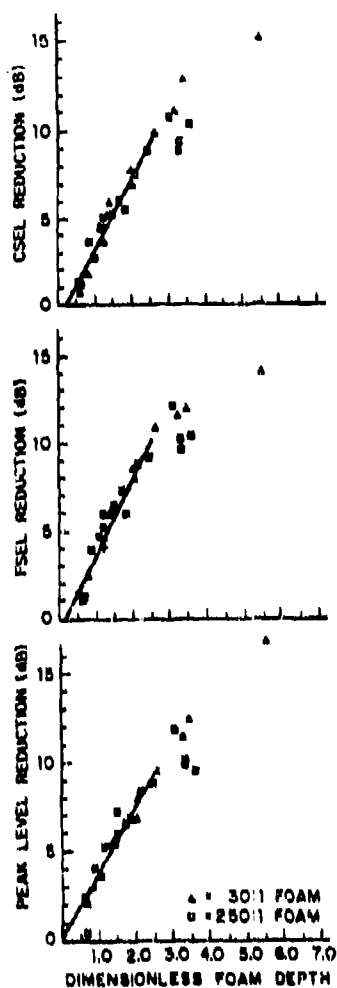


Fig. 3. Reductions versus dimensionless foam depth for $\alpha=30$ and $\alpha=250$ foam (from Ref. [1]). Dimensionless foam depth is defined in eqn. (3) of the text.

water components do not achieve immediate equilibrium. This lessens the degree of attenuation.

Much work has been done to explain the effectiveness of foam as a shock attenuator [2-4]. These works include theories based on multiple reflections from bubble surfaces and broadening of the shock due to bubble resonances. It should be noted that these mechanisms only occur in the acoustic or near acoustic range of overpressure and are probably not applicable to the extremely large overpressures encountered in explosively initiated shock waves. It was pointed out by Raspet and Griffiths [1] that the minimum shock strength needed to shatter the foam structure is on the order of several hundred kPa.

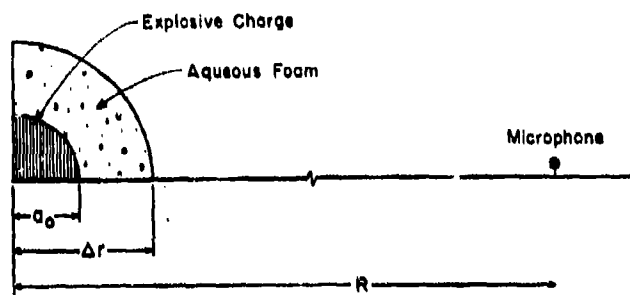


Fig. 3. Schematic of explosive/foam configuration.

Other experiments [5,6] have cited the vaporization of the water and the quenching of the afterburn as mechanisms which reduce the delayed energy imparted to the wave. We believe that the energy contribution by afterburn is a small percentage of the energy delivered by the initial detonation wave and is probably not the main mechanism for attenuation. The effects of vaporization will be examined in more detail later in this study.

The work presented here is by no means a detailed study of the pore surface structure within the foam. Instead, emphasis is placed on the hydrodynamic wave interactions within the medium and between material interfaces. Based on the strength of the explosively driven shock wave through the foam, the hydrodynamic model appears to be a valid approach. The following sections will outline the problem analysis, numerical solution technique and some results.

Analysis

Figure 3 defines the problem at hand. Located at the $r=0$ origin is a spherical charge of explosive with radius a_0 . Surrounding the explosive is a foam with expansion ratio α and depth Δr . Surrounding the foam is air. For this analysis, the initial time is taken as the instant the detonation wave reaches the explosive/foam interface ($r=a_0$). The form of the detonation wave at this time is assumed to be the classical form of Taylor [7] for a spherical self-similar detonation wave profile. The magnitude of the transmitted and reflected waves at the foam boundary are calculated from the Rankine-Hugoniot jump conditions and the equations of state for the two materials (explosive, foam). In order to study the wave motion beyond this initial time, one must solve the equations of motion, equations of state, and the appropriate boundary and initial conditions for the entire flow field. For a one-dimensional, spherically symmetric analysis the equations of motion in Eulerian form are written as

Conservation of mass

$$\frac{\partial \rho}{\partial t} + u \frac{\partial \rho}{\partial r} + \rho \frac{\partial u}{\partial r} + 2 \frac{\rho u}{r} = 0 \quad (4)$$

Conservation of momentum

$$\frac{\partial u}{\partial t} + u \frac{\partial u}{\partial r} + \frac{1}{\rho} \frac{\partial P}{\partial r} = 0 \quad (5)$$

Conservation of energy

$$\frac{\partial E}{\partial t} + u \frac{\partial E}{\partial r} - \frac{P}{\rho^2} \left(\frac{\partial \rho}{\partial r} + u \frac{\partial \rho}{\partial t} \right) = 0 \quad (6)$$

Equation of state

$$E = E(P, \rho) \quad (7)$$

At $r=0$ a reflected boundary condition is imposed and at $r=R$ a transmitted boundary condition is used. Internal boundary conditions at the material interfaces require continuity of particle velocity, u and pressure.

Along with appropriate initial conditions, the three nonlinear partial differential equations and the equation of state form a set of four equations to be solved for the four unknown variables E , P , u , and ρ . In order to obtain an analytical solution to this set of equations, some very limiting assumptions must be made [8-13]. A review of much of this work can be found in Ref. [14].

The solution technique used in the work performed here is based upon the finite difference solution to the governing differential equations and constitutive relations. A brief discussion of the solution technique follows.

Finite difference solution

The finite difference code used to solve the blast attenuation processes is an adaptation of the one-dimensional WONDY V code developed at Sandia Laboratories [15]. A detailed description of the operation of the code can be found in Ref. [15]. A brief discussion of the computational scheme, stability and ideal form of the state equation will be presented here.

The finite difference code is used to solve the set of one-dimensional equations of motion in spherical geometry. The governing equations written in Lagrangian form are

Conservation of mass

$$m = m_0 \quad (8)$$

Conservation of momentum

$$\rho a = - \frac{\partial P}{\partial x} - \frac{\partial q}{\partial x} \quad (9)$$

Conservation of energy

$$\rho \frac{\partial E}{\partial t} = (P+q) \frac{1}{\rho} \frac{\partial \rho}{\partial t} \quad (10)$$

Equation of state

$$P = P(E, \rho) \quad (11)$$

Here, m represents the mass, ρ is the density, q is a viscous stress, P is the pressure, and E is the specific internal energy.

In the finite difference approximation to the differential equations all quantities sampled are material particles at discrete times. The differential equations are written in difference form by the use of centered, second-order analogs over a staggered computational grid. The space variables, a , u , and x (acceleration, velocity, and spatial location) are located at the cell boundaries, and the thermodynamic variables, P , E and ρ are centered in each cell.

Since the grid resolution of the code cannot be made small enough to accurately resolve the shock waves thickness, an apparent viscous stress q is introduced. This prevents the wave form from overtaking itself and increases computational stability by spreading the discontinuity across several cells. Shock waves in the finite difference solution are recognized as very steep but finite gradients in the solution. The form of q used in this work is

$$q = C_1 C_s \frac{\partial \rho}{\partial t} + C_2 \rho \left(\frac{1}{\rho} \frac{\partial \rho}{\partial t} \right)^2 \quad \text{if } \frac{\partial \rho}{\partial t} > 0 \quad (12a)$$

$$q = 0 \quad \text{if } \frac{\partial \rho}{\partial t} < 0 \quad (12b)$$

Here, C_1 and C_2 are constants [15] and C_s is the local sound velocity. In addition to providing numerical stability, the apparent viscous stress also satisfies the entropy production across the shock front as dictated by the second law of thermodynamics.

Equation of state for aqueous foam

When a shock passes through a liquid-gas mixture, the liquid requires a finite time to equilibrate velocity and temperature with the gas. In the relaxation zone, differences in velocity and temperature between the phases cause momentum and heat transfer which can have important effects on the resulting two-phase flow field. Often these processes proceed very rapidly, particu-

larly when one phase is finely dispersed in the other. When this happens it can be assumed that equilibrium is reached at the shock front and that the two component systems can be considered as a homogeneous pseudofluid that obeys the usual equations of single component flow.

As stated earlier, aqueous foam consists of a matrix of thin sheets of water encapsulating small pockets of air. In this analysis it is assumed that when a strong shock hits these thin sheets they are shattered into microdroplets by the viscous stress across the shock plane. This assumption is elaborated in Ref. [1]. Because of the droplets' size, they equilibrate very rapidly with the flowing gas. This assumption enables one to consider the system as an homogeneous entity, and thus use mass averaged thermodynamic properties to describe the system. These properties are weighted averages and are not necessarily the same as the properties of either phase. Pore surface structure is not treated in this work because of the strong shock overpressures.

In order to analyze shock propagation through foam using a finite difference method, one must first develop an equation of state for the homogeneous pseudofluid using average properties of the air and water components. The equation is then put in a form most amenable to hydrocode calculation, namely eqn. (11).

The task here is to find the fluid pressure given the fluid density and fluid internal energy using both the ideal gas equation of state with a nonconstant specific heat for air and an equation of state for water of the form $[P, E] = f(T, v)$. The water equation of state was supplied by Sandia Laboratories [15] and was found to be consistent to the fifth significant digit when compared with tabulated values from steam tables by Keenan, Keyes, Hill and Moore [16].

The equilibrium solution is found by satisfying the mixture mass (volume) and energy relations

$$\text{mixture energy} \quad E_f = xE_a + (1-x)E_w \quad (13a)$$

$$\text{mixture mass} \quad v_f = xv_a + (1-x)v_w \quad (13b)$$

where x = mass fraction of air, E = specific internal energy, and v = specific volume.

The subscripts f , a and w stand for fluid mixtures, air and water, respectively. In addition, we have the functional relations

$$E_a = f(T) = E_a(T) \quad (14a)$$

$$E_w = f(T, v_w) = E_w(T, v_w) \quad (14b)$$

$$v_a = RT/P_a \quad (14c)$$

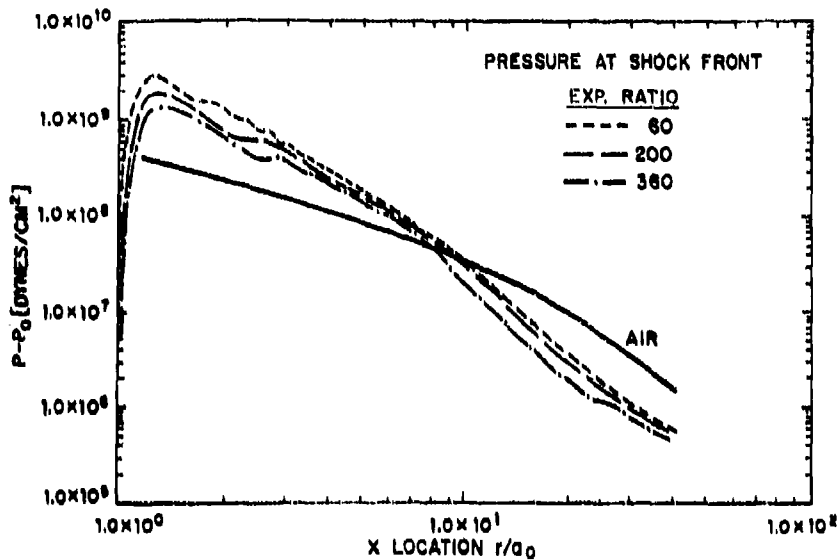


Fig. 4. Shock overpressure for various expansion ratio foams. For all cases, $\Delta r/a_0 = 40$.

$$P_w = f(T, v_w) = P_w(T, v_w) \quad (14d)$$

Assuming that the pressure and temperature of both phases are equal, we can rewrite the mass and energy relations as

$$E_f = xE_a(T) + (1-x)E_w(T, v_w) \quad (15a)$$

$$v_f = x \frac{RT}{P_w(T, v_w)} + (1-x)v_w \quad (15b)$$

The two equations are coupled through the fluid temperature, T , and the water specific volume, v_w . This provides two equations in two unknowns, T and v_w . The solution will yield the fluid pressure through the water equation of state, $P_w(T, v_w)$.

Since the internal energy of water is dependent on both temperature and specific volume (due to phase change) the temperature cannot be solved directly from the energy equation. If this were the case, pressure could be solved for by satisfying the mass relation, varying v_w . Since this is not possible, an iterative scheme must be employed to solve the two equations simultaneously.

Computed results

Figure 4 is a plot of the peak shock pressure as a function of distance from the charge center $r=0$. Three different expansion ratio foams (60, 200, 360)

are shown in the figure. Each case illustrated in Fig. 4 has a foam depth of $\Delta r/a_0 = 40$. Figure 4 also includes a plot of the locus of the peak shock pressure in an air medium (no foam $\alpha = \infty$) for the same charge [11]. The general trend is for the lower expansion ratio foams to start at a higher shock pressure than the air and higher expansion foams. The higher initial shock pressures for the lower expansion ratio foams is a result of the foam shock impedance and the product gas/foam interface boundary condition. Figure 4 also shows a break in the rate of pressure decrease at about 8 charge radii for the 60:1 foam; 9 charge radii for the 200:1 foam; and 10 charge radii for the 360:1 foam. The rate of pressure decay increases after this point. Evaluation of the thermodynamic properties shows that this break occurs when the lead shock is no longer of sufficient strength to vaporize the foam. This attenuation mechanism becomes evident when studying the pressure, energy and velocity histories of the attenuating flow fields.

Figures 5-7 show pressure, energy and density profiles for a constant expansion ratio (200:1) foam where the foam depth is 10 charge radii. In all six different depths were studied 5, 10, 15, 20, 30 and 40 charge radii, with the solutions integrated to a distance of 90 charge radii. Thermodynamic profiles for the remaining cases are not shown here, but can be found in Ref. [14]. These calculations were performed in order to investigate the blast wave behavior at the foam/air interface and to observe the effects of different foam depths on the far field wave form. The initial blast wave for these calculations was determined from an equation of state for TNT used by Brode [13] starting at the initial conditions specified by Taylor [7].

The results shown in Figs. 5-7 show the radial distance scaled to the initial charge radius. Pressure is scaled to ambient pressure (0.101 MPa) and density, energy and time are left unscaled. Also τ represents the elapsed time (μs) since the detonation wave reached the explosive/foam interface. It should be noted that prior to solving the flow equations with foam as the propagation medium, a test case was run for a standard charge in dry air. This particular test of the finite difference code was made since the corresponding experimental results are well documented [17]. The peak overpressures for this case were in favorable agreement with experimental observations in both the near-field and far-field.

Examining the results shown in Figs. 5-7, one can see that there is no significant difference in the pressure profiles other than that the second shock is attenuated more and is farther into the positive region as the depth increases. This does not explain the change in the rate of attenuation. However, inspection of the internal energy variations offers an explanation of the phenomena.

The increase in internal energy above the ambient is the last influence that the blast wave produces. The kinetic and thermal energy of the initial explosive products that goes into producing the blast wave will be distributed in the final state as an increase in the internal energy of the surrounding medium. When

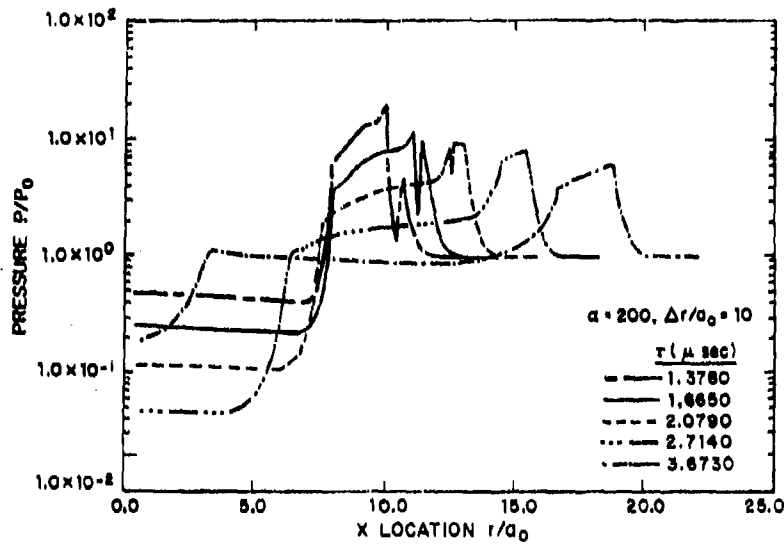


Fig. 5. Shock overpressure history for 200:1 expansion ratio foam, $\Delta r/a_0 = 10$.

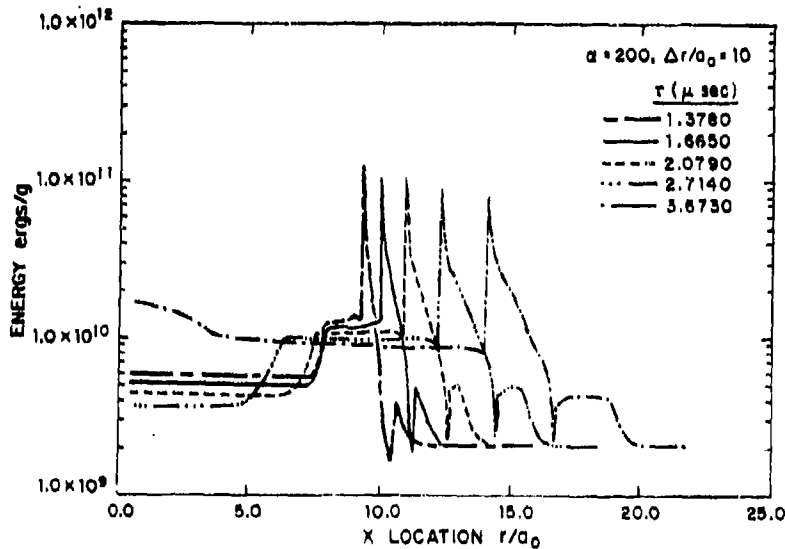


Fig. 6. Specific internal energy history for 200:1 expansion foam, $\Delta r/a_0 = 10$.

the shock wave passes a given location, it leaves the material at a pressure and energy determined by the jump conditions and the equation of state. When the medium expands back to ambient pressure, it returns some of this energy to the wave propagating ahead of it and retains some residual energy as a result of the irreversible heating caused by molecular shearing across the shock front. As the strength of the shock diminishes, the residual energy also diminishes.

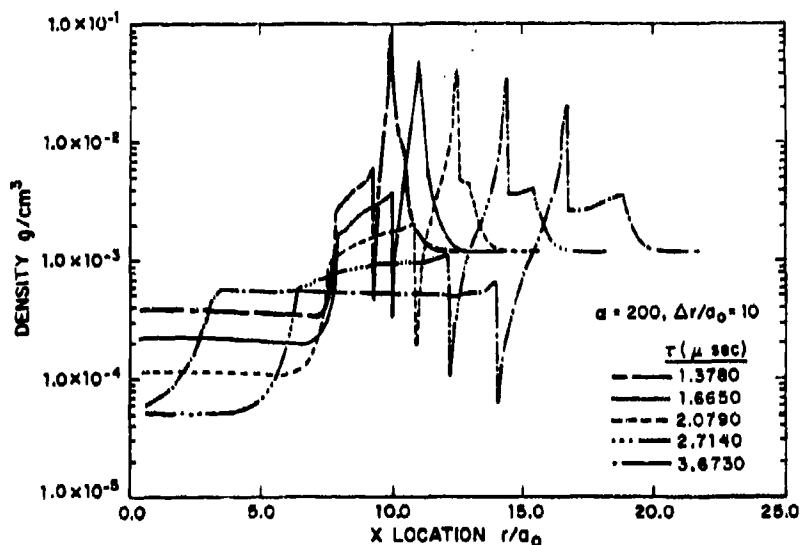


Fig. 7. Density history for 200:1 expansion ratio foam, $\Delta r/a_0 = 10$.

In this weak shock case the wave can be thought of as propagating acoustically with the attenuation mostly due to spherical divergence. The spike in the internal energy-distance plots (Fig. 7) is due to the density discontinuity occurring at the material interface.

In order to make a comparison of the computed foam depth attenuation effectiveness with the data reported by Ref. [1], the data shown in Fig. 8 are presented as *reduction in dB* peak level in Fig. 9. Here, the dB reduction is relative to the overpressure predicted for an r/a_0 of zero. Figure 8 shows this to be 185.8 dB. Thus, for example, a normalized foam depth of 10 would give a dB reduction of $185.8 - 183.2 = 2.6$. The predicted dB reductions for five different cases of r/a_0 are shown in Fig. 9. Also shown (as a solid line) for comparison is the measured far-field peak level dB reduction for an $\alpha = 250$ foam, taken from Fig. 3 of Ref. [1].

A least-squares fit of the predicted Peak Level Reduction (PLR)_{dB} for normalized foam depths less than 25 is,

$$(\text{PLR})_{\text{dB}} = 0.28 (\Delta r_{\text{foam}}/a_0) - 0.04 \quad (16)$$

In order to compare this with the data presented in Ref. [1] (as shown in Fig. 9) it was necessary to first carry out some conversions, since the data (Fig. 3 of Ref. [1]) are presented as (PLR)_{dB} versus scaled foam depth ($r/M^{1/3}$). This depth is the ratio of foam depth divided by the cube root of the explosive charge mass. In terms of that parameter, the best-fit equation for the $\alpha = 250$ foam was a far-field dB reduction that is given by

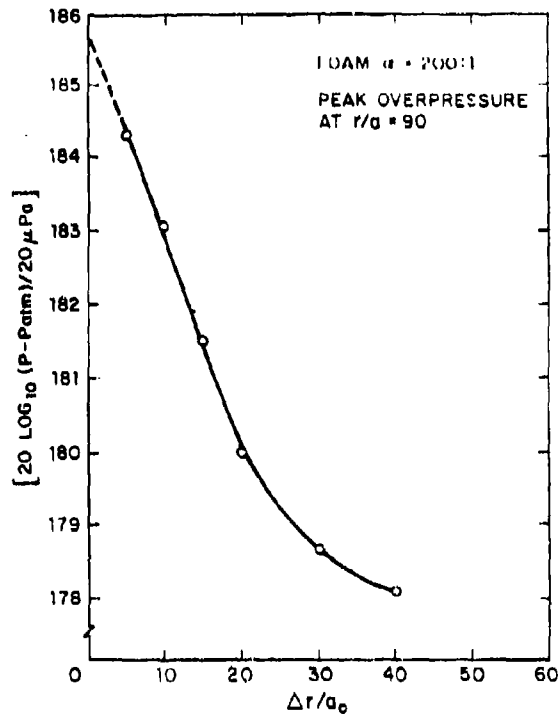


Fig. 8. Predicted "far-field" overpressure decibel level as a function of normalized foam thickness ($\alpha = 200$ foam).

$$(\text{PLR})_{\text{dB}} = 6.33 (\Delta r_f / M^{1/3} - 0.03) \quad \text{for } 0 \leq \Delta r_f / M^{1/3} \leq 1.5 \quad (17)$$

Since the explosive used in the experiments was C-4, not TNT, it was necessary to scale the mass of C-4 to an equivalent TNT mass of TNT, $M_{\text{TNT}} = 1.35 M_{\text{C-4}}$. Therefore, to determine the equivalent charge radius, a_0 (as used in the computer prediction)

$$M_{\text{C-4}}^{1/3} = (M_{\text{TNT}} / 1.34)^{1/3} = 1.73 (4\pi \rho_{\text{TNT}} / 3)^{1/3} a_{\text{OTNT}} \quad (18)$$

Thus 1 kg of C-4 explosive is equivalent to a mass of TNT with $a_{\text{OTNT}} = 0.04$ m.

When substituting this relation into eqn. (17) one obtains the experimental best least-squares fit, as

$$(\text{PLR})_{\text{dB}} = 0.366 (\Delta r_f / a_0) - 0.19 \quad \text{for } 0 \leq r/a_0 \leq 26 \quad (19)$$

This equation is shown by the solid line in Fig. 9 and compares favorably with eqn. (16).

Conclusions

The results presented show an increase in the rate of attenuation after the shock no longer vaporizes the water component of the mixture, leading one to

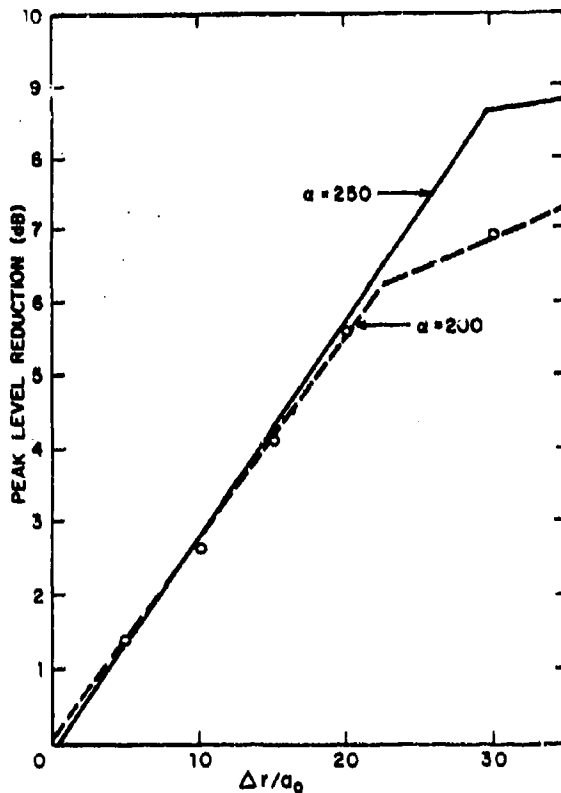


Fig. 9. Comparison of the predicted decibel peak level reduction (in the "far-field") with experiments from Ref. [1] (solid line).

conclude that vaporization can in fact be detrimental to maximum attenuation. When the liquid component of the system vaporizes, the air is no longer loaded with a relatively incompressible material and the shock speed increases. This enables secondary shocks to catch up to and reinforce the main shock. This aspect of phase change is also detrimental to attenuation in the intermediate field. The greater propagation speed of the secondary shocks may also account for the reduced duration of the negative phase.

The many wave reflections off the foam/air interface produce a complicated waveform in this region. However, it was noted that these disturbances rapidly decay into the air region and are small compared to the peak disturbance. For smaller foam depths the transmitted pressure is still high, and nonacoustic attenuation by the air adjacent to the foam occurs.

A significant pressure drop occurs at the foam/air interface for small foam depths, and in this respect, the impedance mismatch between the air and the foam is important. However, for large foam depths, where the attenuation due to shock dissipation occurs solely in this region, the effects of reflections from

the foam/air surface and the impedance mismatch have little influence on the far field waveform.

Two factors are responsible for determining the amount of residual heat left in the medium once the shock has passed. One is the thermodynamic properties that influence the conditions across the shock discontinuity. For maximum attenuation (for a given pressure) one would wish to maximize the rise in internal energy across the shock and minimize the drop in energy during isentropic expansion back to ambient pressure. This effect is determined solely by the equation of state of the medium. The other contributing factor is that, for the same material, a higher pressure shock produces a larger amount of residual energy. Thus, for large foam depths where interface interactions are minimal, the two most important factors contributing to high attenuation are a maximum initial overpressure and the ability to produce a high residual energy. In addition, the lower expansion ratio foams attenuate more than light foams for two possible reasons. The first is that the initial overpressure is higher and the second is that for a given pressure, more residual energy is produced. It is likely that both factors contribute.

Beyond a certain foam depth the amount of residual energy left in the region of expanded foam drops sharply. Most of the energy imparted to the foam by the shock is then returned to the wave upon expansion. Attenuation past this point is due mostly to divergence.

Acknowledgement

The authors acknowledge Dr. Stewart Griffiths, Sandia National Laboratories, Albuquerque, NM, for his input into the equation of state analysis.

References

1. R. Raspet and S.K. Griffiths, The reduction of blast noise with aqueous foam, *J. Acoust. Soc. Amer.*, 74(6) (1983) 1757-1763.
2. D.L. Evans, D.F. Jankowski and E.D. Hirleman, A preliminary investigation of aqueous foam for blast wave attenuation, ERC-R-78050, College of Engineering and Applied Sciences, Arizona State University, Tempe, AZ, January 1979.
3. J.S. de Krasinski and A. Khosla, Shock attenuation in non-homogeneous and porous media, Report No. 34, University of Calgary, Canada, Department of Mechanical Engineering, March 1972.
4. V. Ramesh and J.S. de Krasinski, Shock and flame tube laboratory experiments, Report No. 73, University of Calgary, Canada, Department of Mechanical Engineering, March 1976.
5. A.K. Clark, P.J. Hubbard, P.R. Lee and H.C. Woodman, The reduction of noise levels from explosive test facilities using aqueous foams, NSW/WO2 TR 77-36, NSWL, July 1977.
6. D.A. Dudley, E.Q. Robinson and V.C. Pickett, The use of foam to muffle blast from explosions, Paper presented at the IBP-ABCA Meeting, June 1976.
7. G.I. Taylor, The dynamics of the combustion products behind plane and spherical detonation fronts in explosives, *Proc. R. Soc. London, Ser. A*, 200 (1950) 235.

- 8 G.I. Taylor, The air wave surrounding an expanding sphere, Proc. R. Soc., London, Ser. A, 186 (1946) 273-292.
- 9 A.H. Taub (Ed.), John Von Neumann Collected Works, Vol. VI, Pergamon Press, New York, 1963.
- 10 L.I. Sedov, Similarity and Dimensional Methods in Mechanics, Academic Press, New York, 1959.
- 11 S. Griffiths, Aqueous foam blast attenuation, internal report, Sandia Laboratories, New Mexico; Private communication to Professor Herman Krier and Dr. Richard Raspet, September 1982.
- 12 S.R. Brinkley and J.G. Kirkwood, Theory of the propagation of shock waves, Phys. Rev. 71(9) (1947) 606-611.
- 13 H.L. Brode, Blast wave from a spherical charge, Phys. Fluids, 2(2) (1959).
- 14 T.D. Panczak and H. Krier, Shock propagation and blast attenuation through aqueous foams, UILU ENG 83-4007, University of Illinois, 1983.
- 15 M.E. Kipp and R.J. Lawrence, WONDY V — A one-dimensional finite-difference wave propagation code, SAND81-0939, Sandia Laboratories, NM, June 1982.
- 16 J.H. Keenan, F.G. Keyes, P.G. Hill and J.G. Moore, Steam Tables, John Wiley & Sons, New York, 1969.
- 17 W.E. Baker, Explosions in Air, University of Texas Press, Austin, 1973.

The Effect of Material Properties on Reducing Intermediate Blast Noise

R. Raspet

US Army Construction Engineering Research Laboratory, Champaign,
Illinois (USA)

P. B. Butler* and F. Jahani

Department of Mechanical Engineering, The University of Iowa,
Iowa City, Iowa 52242 (USA)

(Received 1 May 1986; revised version received 6 November 1986;
accepted 10 November 1986)

SUMMARY

This work investigates the effectiveness of several different materials on the reduction of blast noise produced by detonating high explosives. In each case, the explosive charge is centered in a cube of blast reducing material. The materials selected have quite different physical properties (e.g. steel wool, straw and plastic bubble pack) and hence, the results provide some insight into the dominant mechanism for energy transfer between the shocked air and the blast reducing materials. In all cases reported, the flat-weighted sound exposure level (FSEL), C-weighted sound exposure level (CSEL), and the peak sound level (P_p) were measured at four positions, 2 at 38 m and 2 at 76 m. Based on the experimental data presented, all four materials tested scaled as a function of the geometrically averaged material depth, the material density and the explosive masses (kg-TNT equivalent). Furthermore, in all cases studied the peak level scales more exactly than do the energy integrals CSEL and FSEL.

INTRODUCTION

It has been recognized for some time that the intense sound levels produced by detonating high explosives can be hazardous for the surrounding

* To whom all correspondence should be addressed.

Applied Acoustics 0003-682X/87/\$03.50 © Elsevier Applied Science Publishers Ltd, England, 1987. Printed in Great Britain Used with permission.

environment. With many of the ordnance test and disposal sites being slowly encroached upon by ever-expanding nearby communities, the task of blast noise reduction takes on growing importance. For the past several years the Acoustics Team at the U.S. Army Construction Engineering Research Laboratory (USACERL) has been investigating blast wave attenuation. Much of the work emphasized reducing the blast energy while it is still within several charge radii of the source. One approach is to surround the explosive charge with an energy absorbing heterogeneous material (e.g. aqueous foam, fibrous materials, granular materials). In brief, a multiphase medium aids blast attenuation through increased energy dissipation.

Several papers over the recent years¹⁻³ have reported on the use of both high and low expansion ratio ($V_{\text{air}}/V_{\text{liquid}}$) aqueous foams as blast-reducing agents. The foam referred to in these papers is generated by means of a batch foamer and is similar in composition to those used in fire fighting. Raspet and Griffiths¹ reported experiments showing the aqueous foam acts as a fairly good blast-reducing agent. Numerical calculations presented by Panczak, Butler and Krier² illustrate the effect of the water droplet vaporization on the overall attenuation process. It was concluded in Ref. 2 that the post-shock vaporization of the water is actually detrimental to maximum attenuation. This observation is contrary to the speculations made in previous work on attenuation of blast waves in foam. Evans, Jankowski and Hirléman³ suggested that for certain expansion ratio foams, mass loading is the principal factor in attenuation. More recent work by Powers and Krier⁴ reported on the attenuation effectiveness of detonating the explosive charges in an open pit as opposed to the open atmosphere. This work was carried out in order to optimize the pit geometry for blast noise reduction.

The work presented in this paper will focus on the effect several energy-absorbing heterogeneous materials have on the reduction of intermediate field (i.e. > 150 dB) blast noise. Test data for several different materials are presented. The materials selected have quite different physical properties (e.g. steel wool, fiberglass, straw and plastic bubble pack) and hence, the experimental results should provide some insight into the dominant mechanism for energy transfer between the shocked air and the blast-reducing materials. In all cases reported, the flat-weighted sound exposure level (*FSEL*), C-weighted sound exposure level (*CSEL*), and the peak sound level (*PEAK*) were measured at four positions in the farfield, 2 at 38 m and 2 at 76 m. The exact locations relative to the explosive charge are shown in Fig. 1. A total of 24 different configurations were tested with 3-4 repetitions for each configuration. The parameters varied in the test were the mass of explosive driver, the mass and type of attenuation material, and the depth of attenuation material.

Reducing intermediate blast noise

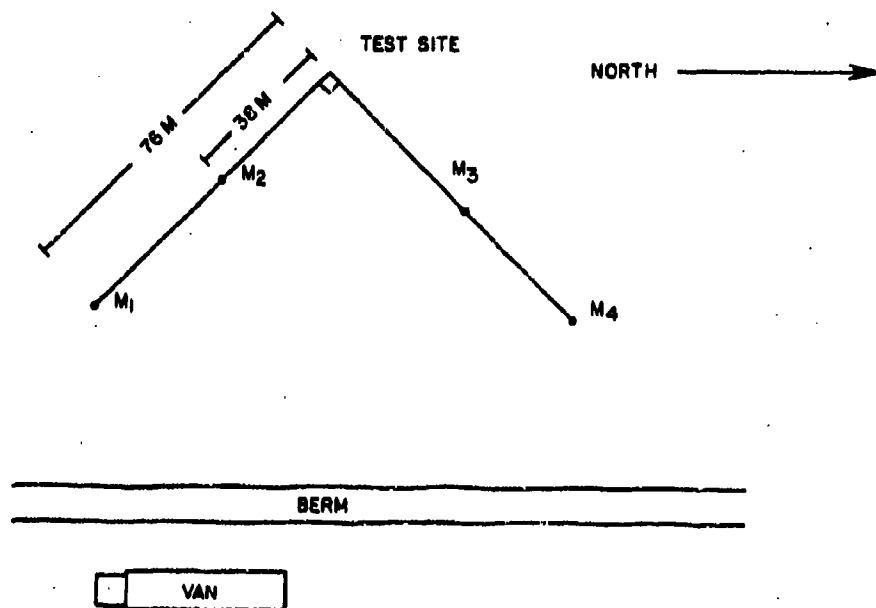


Fig. 1. Microphone layout for test range 33, Fort Leonard Wood. The microphone locations are indicated as M_1 , M_2 , M_3 , and M_4 .

Although the data are somewhat limited in the range of charge mass, experimental results indicate that the noise reduction produced by the four materials scales reasonably well with the dimensionless material depth X^* developed for the study of aqueous foam.¹ This scaling parameter (X^*) includes attenuation effects due to the material thickness, apparent material density, and mass of the explosive driver. In some cases presented, there is evidence that noise reduction is also dependent on fiber size. However, when data from all four materials are combined, the fiber-size dependency appears to be secondary when compared to the mass loading effect. These data are presented in the following sections along with a brief description of the test procedure.

TEST PROCEDURE

All measurements were performed using the same experimental layout (Fig. 1). Endeavor piezo-resistive microphones were used with CERL-constructed line drivers. The microphones were mounted on tripods 1.2 m above ground level. They are indicated in Fig. 1 by M_1 - M_4 . Lines were run from the microphones to the equipment van for recording and analysis. The C-weighted sound exposure level, the flat-weighted sound exposure level, and

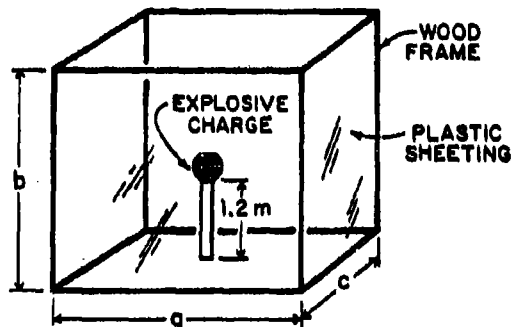


Fig. 2. Schematic of structure used to confine the blast attenuation materials. In all cases, $a = b = c$ (3 ft or 4 ft).

the peak level were measured with a CERL True Integrating Environmental Noise Monitor and Sound Exposure Level Meter for each station, and the signals recorded on an Ampex 2230 14-track FM recorder. By definition, the sound exposure level is given as

$$SEL = 10 \log \left[\int P^2 dt / P_0^2 t_0 \right] \quad (1)$$

where P_0 and t_0 are reference pressure (20 μ Pa) and time (1 s), respectively. Peak pressure is defined in terms of a decibel level (dB)

$$PEAK = 20 \log_{10} [(P_p - P_0) / P_0] \quad (2)$$

where P_p is the measured peak pressure (Pa). The above-mentioned instruments were calibrated before each test using a Bruel and Kjaer pistonphone and the calibration was rechecked after the test.

A wood frame structure with covering made of lightweight polyethylene plastic sheeting (Fig. 2) was used to hold the blast-reducing material in place prior to detonating the explosive. This arrangement is similar to the one used by Raspet and Griffiths¹ in their previous work, in which both high and low expansion ratio aqueous foams were used as the blast-reducing material. In the experiments reported here, the polyethylene cubes were either 0.765 m³ (27 ft³) or 1.812 m³ (64 ft³) in volume. The explosive material was C-4, a commonly used plastic explosive with an effective energy yield approximately 1.36 times that of TNT. Calculated detonation properties for C-4 are presented in Table 1. In all firings, either 0.5 stick or 1 stick (0.57 kg) of C-4

TABLE 1
Detonation Properties of C-4 Explosive³

| | |
|----------------------------------|-------------------------------|
| Detonation velocity (CJ) | 8.37 mm μ s ⁻¹ |
| Detonation pressure (CJ) | 25.7 GPa |
| Bulk density of material | 1.66 g cm ⁻³ |
| Heat of detonation (theoretical) | 5.86 MJ kg ⁻¹ |

was used as the blast source. In order to minimize ground effects, the explosive charge was mounted on a vertical post in the center of the cubic structure. The enclosing structure was completely filled with one of the blast-reducing materials and the charge was detonated remotely. The polyethylene and wood enclosure was chosen since it is rigid enough to support the heavier materials (i.e. 40 kg of steel wool), yet does not offer enough resistance to act as an additional attenuation mechanism.

TEST RESULTS

Four different blast-reducing materials were chosen for this series of tests. They consisted of steel wool, fiberglass, straw and a plastic bubble pack commonly used for packaging and shipping delicate items. Two different grades of the steel wool were used, #0000 grade with a fiber diameter (d) of approximately $150\ \mu\text{m}$, and #3 grade with an effective fiber diameter of $240\ \mu\text{m}$. The #0000 grade has a circular cross-section, while the #3 grade is more rectangular. Both were produced in roll form as opposed to pads. The two different grades will be referred to as fine and coarse steel wool, respectively, in the tables and figures to follow. Steel wool was chosen as a potential blast-reducing material for four primary reasons, the high density, high heat capacity, high thermal conductivity and high surface-to-volume ratio of the fibers. Theoretically, all four of these features should aid in the blast attenuation through increased two-phase energy transfer between the shocked gas and the solid material.

The fiberglass was also tested in two different sizes, a fine grade ($d = 5\ \mu\text{m}$) and a coarse grade ($d = 10\ \mu\text{m}$). It has a density about $1/3$ of steel and a specific heat about twice that of steel, and hence should have different attenuation properties. In addition, the thermal conductivity is significantly different from that of steel wool. The two different fiber diameters were chosen in order to study the effect of specific surface area on blast reduction. In addition to the steel wool and fiberglass, one grade of straw with an external diameter of approximately $2.5\ \text{mm}$ was tested, and the bubble pack was tested for two different bubble sizes ($d = 14.5\ \text{mm}$ and $d = 29.0\ \text{mm}$). Straw was selected since at least one U.S. Army installation has used straw as a noise reducing material.⁶ It should be noted that the straw was cellular in structure with an approximate internal diameter of $50\ \mu\text{m}$. Because of the cellular structure of straw, it was difficult to determine the exact surface area exposed to the flow of hot product gases from the detonation. In summary, Table 2 lists the materials investigated along with some of the physical properties we feel play a key role in analyzing blast wave attenuation.

Table 3 summarizes the test results. Listed for each experiment is the mass

TABLE 2
Blast-reducing Material Properties^{a, b}

| Material description | Material number | Diameter (μm) | Density (kg m ⁻³) | Conductivity (W m ⁻¹ K ⁻¹) | Specific heat (J kg ⁻¹ K ⁻¹) |
|----------------------|-----------------|---------------------|-------------------------------|---|---|
| Steel wool (fine) | #1 | 150 | 7750 | 60.6 | 459 |
| Steel wool (coarse) | #3 | 240 | 7750 | 60.5 | 459 |
| Bubble pack (small) | #3 | 14 500 ^a | 930 | 0.38 | 1430 |
| Bubble pack (large) | #4 | 29 000 ^a | 930 | 0.38 | 1430 |
| Straw | #5 | 50 | 43 | 0.039 | 1340 |
| Fiberglass (fine) | #6 | 5 | 2500 | 0.036 | 961 |
| Fiberglass (coarse) | #7 | 10 | 2500 | 0.036 | 961 |

^a This dimension represents the single bubble diameter. The material has a thickness of 0.1 mm.

TABLE 3
Test Data for Blast Wave Attenuation

| Test number | Material* number | ΔPEAK (dB) | ΔCSEL (dB) | ΔFSEL (dB) | Charge† (# stick) | Material mass (kg) | a, b, c‡ (ft) |
|-------------|------------------|------------|------------|------------|-------------------|--------------------|---------------|
| 20 | #1 | 12.1 | 12.6 | 12.2 | 0.5 | 47.67 | 3.0 |
| 38 | #6 | 11.7 | 9.9 | 9.3 | 0.5 | 36.77 | 4.0 |
| 49 | #7 | 11.4 | 8.9 | 9.8 | 1.0 | 37.68 | 4.0 |
| 42 | #5 | 10.9 | 10.6 | 11.1 | 0.5 | 33.14 | 3.0 |
| 47 | #7 | 10.0 | 10.3 | 10.9 | 0.5 | 37.68 | 4.0 |
| 07 | #1 | 9.6 | 10.9 | 11.2 | 0.5 | 29.51 | 3.0 |
| 34 | #6 | 9.3 | 8.0 | 8.2 | 0.5 | 14.53 | 3.0 |
| 40 | #2 | 9.0 | 9.3 | 9.8 | 0.5 | 32.92 | 3.0 |
| 14 | #5 | 8.6 | 8.2 | 6.3 | 1.0 | 68.10 | 4.0 |
| 32 | #3 | 8.4 | 7.4 | 5.7 | 0.5 | 30.42 | 4.0 |
| 01 | #1 | 8.2 | 9.0 | 9.7 | 1.0 | 29.51 | 3.0 |
| 10 | #5 | 8.2 | 8.2 | 9.0 | 0.5 | 29.06 | 3.0 |
| 36 | #6 | 8.1 | 7.3 | 7.8 | 1.0 | 36.77 | 4.0 |
| 09 | #2 | 7.9 | 7.9 | 9.9 | 0.5 | 29.51 | 3.0 |
| 45 | #7 | 7.1 | 7.1 | 7.1 | 0.5 | 14.53 | 3.0 |
| 12 | #5 | 7.0 | 6.4 | 6.3 | 1.0 | 29.06 | 3.0 |
| 04 | #2 | 5.9 | 6.3 | 7.0 | 1.0 | 29.51 | 3.0 |
| 16 | #3 | 5.8 | 4.6 | 4.9 | 0.5 | 16.80 | 4.0 |
| 22 | #2 | 5.1 | 5.4 | 6.2 | 0.5 | 14.76 | 3.0 |
| 25 | #4 | 4.6 | 3.5 | 3.2 | 1.0 | 15.44 | 4.0 |
| 26 | #3 | 4.0 | 3.0 | 3.1 | 1.0 | 18.16 | 4.0 |
| 30 | #3 | 3.9 | 3.2 | 2.0 | 0.5 | 6.36 | 3.0 |
| 28 | #4 | 3.5 | 2.4 | 2.2 | 0.5 | 6.36 | 3.0 |

* See Table 2 for material type.

† One stick C-4 = 0.5675 kg.

‡ Dimension of cubic enclosure.

of explosive material used, mass of attenuation material, the material designation (from Table 2), and the decibel reductions recorded for peak level ($\Delta PEAK$), $\Delta FSEL$ and $\Delta CSEL$. The reductions were determined from the difference between the control charge and the test charge so the variations due to charge mass, compositions, and temperature would be minimized. Where more than one trial occurred, the maximum difference in reduction is listed. From a safety standpoint, the minimum value is probably of more interest. The maximum variation usually occurred for the peak level since this measure is more sensitive to random processes than the integrated measures ($FSEL$ and $CSEL$). On the average, the reduction measured at the closer microphone (38 m) were one to two dB greater than the data measured at the distant microphones (76 m). This difference is due to the more rapid non-linear decay of the unmuffled event. At first glance, Table 3 illustrates several key mechanisms for material attenuation effectiveness. Material mass, depth of material and in some cases material fiber diameter all appear to govern the amount of attenuation a given material produces. These features become more evident when the data are categorized according to material type. With regard to a comparison between different types of materials, it appears that the plastic bubble pack is less effective than the more dense steel wool, straw and fiberglass. These somewhat general observations need to be investigated in more detail.

Figures 3(a)–(c) present the peak level, $FSEL$ and $CSEL$ reductions for the tests where bubble pack was used as the attenuating material. The data for both small (#3) and large (#4) bubble pack are combined on these plots, and although limited in the number of data points, they show good agreement scaled as a function of the dimensionless material depth:

$$X^* = l(\rho_b/C_w)^{1/3} \quad (3)$$

Here, l is the geometrically averaged material depth:

$$l = 0.5(abc)^{1/3} \quad (4)$$

where a , b and c are the enclosure dimensions (see Fig. 2), ρ_b is the material

TABLE 4
Linear Regression Calculations for Bubble Pack (#3, #4):
 $Y = AX^* + B$ Experimental Data

| <i>Y variable</i> | <i>Correlation coefficient</i> | <i>A</i> | <i>B</i> |
|--------------------|--------------------------------|----------|----------|
| $\Delta PEAK$ | 0.98 | 5.0 | -2.87 |
| $\Delta FSEL$ (dB) | 0.97 | 4.0 | -2.80 |
| $\Delta CSEL$ (dB) | 0.96 | 4.7 | -3.38 |

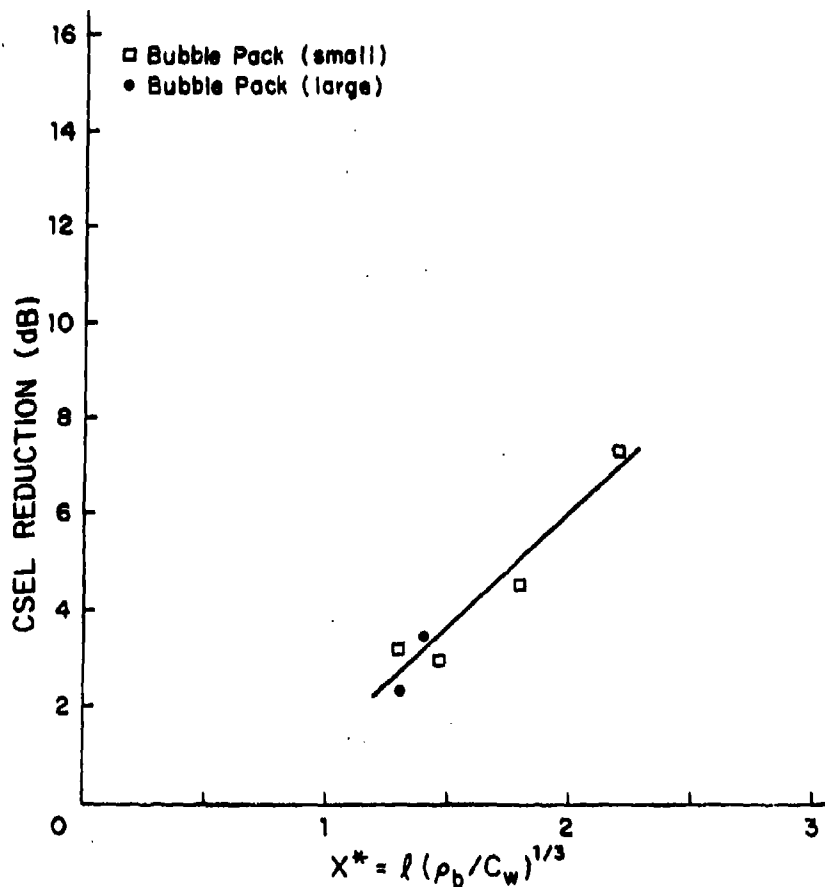


Fig. 3. Noise reductions for two grades of bubble pack. (a).

bulk density (kg m^{-3}) and C_w is the explosive mass (kg-TNT equivalent). The dimensionless material depth given in eqn (3) was used in previous work^{1,2} to scale the attenuation properties of both high and low expansion ratio aqueous foams. It appears to be a fairly representative scaling law that incorporates the material mass, depth and charge weight, all important factors in blast wave attenuation. For bubble pack, there does not appear to be any significant effect of bubble size (#3 vs #4) on the level of attenuation. Table 4 presents the correlation coefficients and linear regression formulas for the three sets of data shown in Figs 3(a)–(c). The bubble pack shows a peak level reduction of about 5 dB per dimensionless material depth, a *FSEL* reduction of 4 dB/ X^* and a *CSEL* reduction of 4.7 dB/ X^* . The previous work with aqueous foam¹ showed reductions of about 4 dB/ X^* for peak, *FSEL* and *CSEL*.

filled with a 30:1 expansion ratio foam produced with a Mearl OT 10 batch foamer. By definition,¹ the expansion ratio is

$$\alpha = V_f/V_l \quad (3)$$

where V_f represents the total volume occupied by the foam, and V_l is the liquid volume. For future comparisons, the test configuration used by Raspet and Griffiths¹ is shown in Fig. 2. Here the aqueous foam is contained in a less-confining plastic cube surrounding the explosive.

In the present investigation, tests were performed with $\frac{1}{2}$ stick of explosives (0.285 kg) in the 0.91-m culvert with two foam depths (0.86 and 0.55 m), and with $\frac{1}{2}$ stick and 1 stick in the 1.22-m diameter culvert with three foam depths (1.16, 0.86 and 0.55 m). One stick of C-4 has a mass equal to 0.57 kg (0.78 kg TNT equivalent). Table 1 contains the results of these tests. In addition to the C-4 mass and foam dimensions (d = diameter, h = height), *CSEL* reduction ($\Delta CSEL$), *FSEL* reduction ($\Delta FSEL$) and peak noise level reduction ($\Delta PEAK$) are listed for the three different combinations of charge size and culvert size.

The *CSEL*, *FSEL* and *PEAK* reductions were determined from the difference between a control charge and the test charge, so that variations due to charge mass, composition and temperature would be minimized. This is the same test procedure as used in Ref. 1.

Three qualitative features of the blast wave reductions can be seen from the results in Table 1. First, increased foam depth for a given culvert and explosive configuration results in increased noise reduction. This feature is evident in the comparison of test 101a with 101b, as well as the comparison of the set including tests 102a, 102b, 102c, 103a, 103b and 103c. A second observation is that an increased culvert diameter for a fixed depth results in greater noise reduction. Finally, increased charge mass results in decreased noise reduction. These dependences are the same as those found in Raspet and Griffiths¹ for unconfined explosives. To display those similarities and

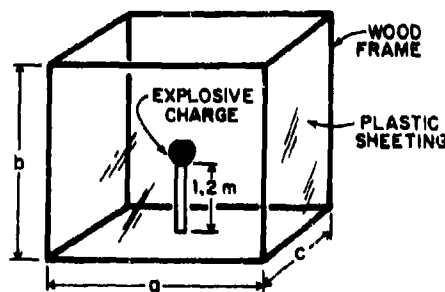


Fig. 2. Schematic of test configuration used by Raspet and Griffiths.¹ Here the foam is confined by plastic sheeting rather than the rigid metal culvert.

Reducing intermediate blast noise

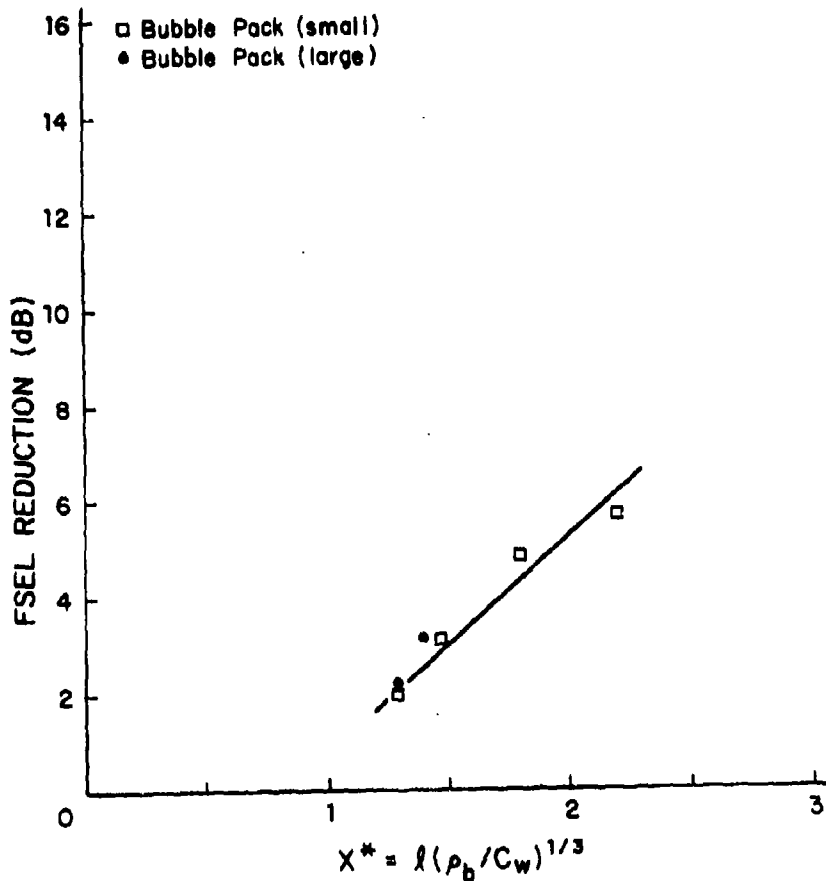


Fig. 3—contd. (b).

Examination of the experimental data for materials #3 and #4 suggests several possible mechanisms for the attenuation of the blast wave as it propagates through the plastic bubble pack. The first is based on a thermal analysis of the plastic material. Since the bubble pack is a combustible material with a relatively high specific surface area, part of the shock wave energy can go into heating up and melting the plastic. Subsequent energy release from the plastic may occur after the wave has propagated well beyond the enclosure volume. Another possibility is that the bubble pack acts to diffract the shock wave as it propagates through the material. This is a result of the shock wave encountering the density discontinuity (impedance mismatch) present in the bubble pack/air matrix. The air within each bubble is at a slightly higher pressure than the surrounding air which fills the voids and hence, there exists a density discontinuity. To determine if the proposed attenuation mechanisms are of primary or secondary significance, the

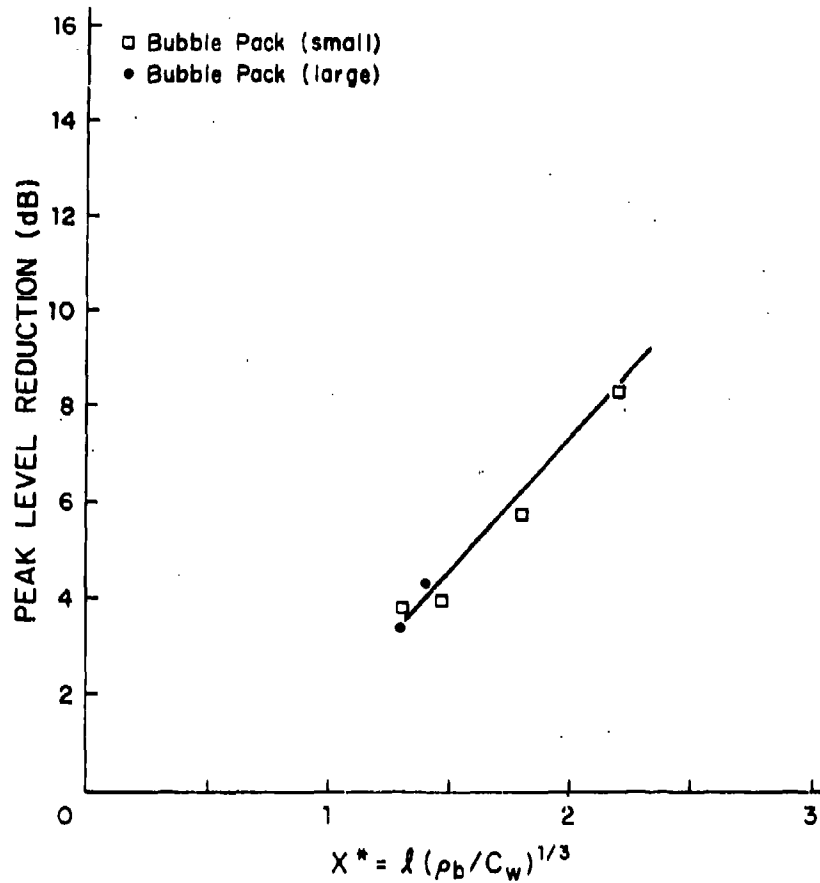


Fig. 3—contd. (c).

attenuation effectiveness of other materials should be examined. For clarity, the data for steel wool (taken from Table 3) are given in Table 5.

Figures 4(a)–(c) display the reductions for the two different grades of steel wool, fine (#1) and coarse (#2). It is interesting to note that the fine and coarse steel wool show slightly different reductions for the same dimensionless material depth (X^*). Taking into account the definition of X^* , this implies that for the same depth of material, mass of material and explosive mass, the two grades of steel wool behaved differently in reducing the blast noise. The only difference between the two is the fiber size, or more specifically the surface-to-volume ratio of the fibers. Recall that both the small and large bubble pack scaled to X^* and hence did not show a dependency of attenuation on a characteristic dimension. This observation at first leads one to consider incorporating a surface area term and possibly a material heat capacity term in the proposed scaling law.

Reducing intermediate blast noise

TABLE 5
Test Data for Steel Wool (from Table 3)

| Test number | Material number | PEAK (dB) | Δ CSEL (dB) | Δ FSEL (dB) | Charge (# stick) | Material mass (kg) | a, b, c (ft) |
|-------------|-----------------|-----------|--------------------|--------------------|------------------|--------------------|--------------|
| 20 | #1 | 12.1 | 12.6 | 12.2 | 0.5 | 47.67 | 3.0 |
| 07 | #1 | 9.6 | 10.9 | 11.2 | 0.5 | 29.10 | 3.0 |
| 01 | #1 | 8.2 | 9.0 | 9.7 | 1.0 | 29.51 | 3.0 |
| 40 | #2 | 9.0 | 9.3 | 9.8 | 0.5 | 32.92 | 3.0 |
| 09 | #2 | 7.9 | 7.9 | 9.9 | 0.5 | 29.51 | 3.0 |
| 04 | #2 | 5.9 | 6.3 | 7.0 | 1.0 | 29.51 | 3.0 |
| 22 | #2 | 5.1 | 5.4 | 6.2 | 0.5 | 14.76 | 3.0 |

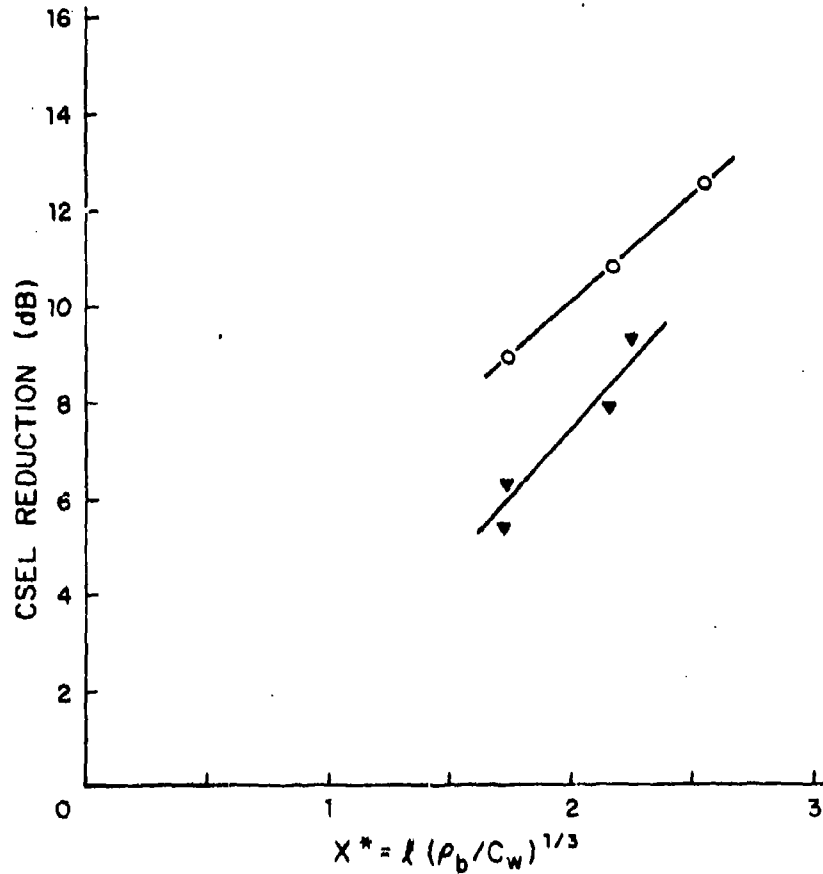


Fig. 4. Noise reductions for two grades of steel wool. \circ , Fine; \blacktriangledown , coarse. Scaled to X^* , the fine grade shows a greater reduction for all metrics. (a).

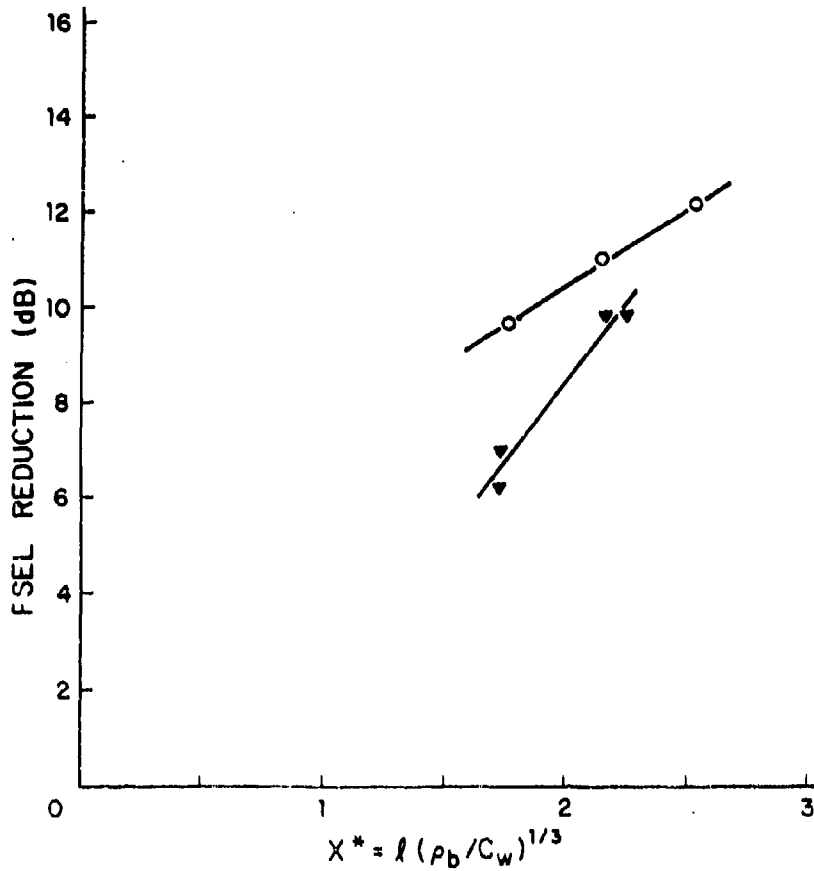


Fig. 4—contd. (b)

With regard to the thermal effects, a lumped parameter heat transfer analysis yields a post-shock thermal equilibration time of 35 ms for the fine fibers and 86 ms for the coarse fibers.⁶ This analysis is based on a 10 MPa shock passing through an air/steel wool two-phase medium. When neighboring fibers are considered, the equilibration times are reduced by a factor of about 20. The quoted equilibration times are only a first-order approximation, but illustrate an interesting point. Because the fine fibers equilibrate with the shocked gases much more rapidly than the coarse fibers, there is a greater decrease in available energy to drive the shock wave through the remainder of the material. However, for a strong shock propagating through steel wool, experimental data⁷ shows that the shock decay time is of the order of 1 ms. Since the predicted equilibration times are of the order of 30–80ms, this implies that heat transfer effects are not important in dissipating the energy. In fact, an adiabatic assumption would

Reducing intermediate blast noise

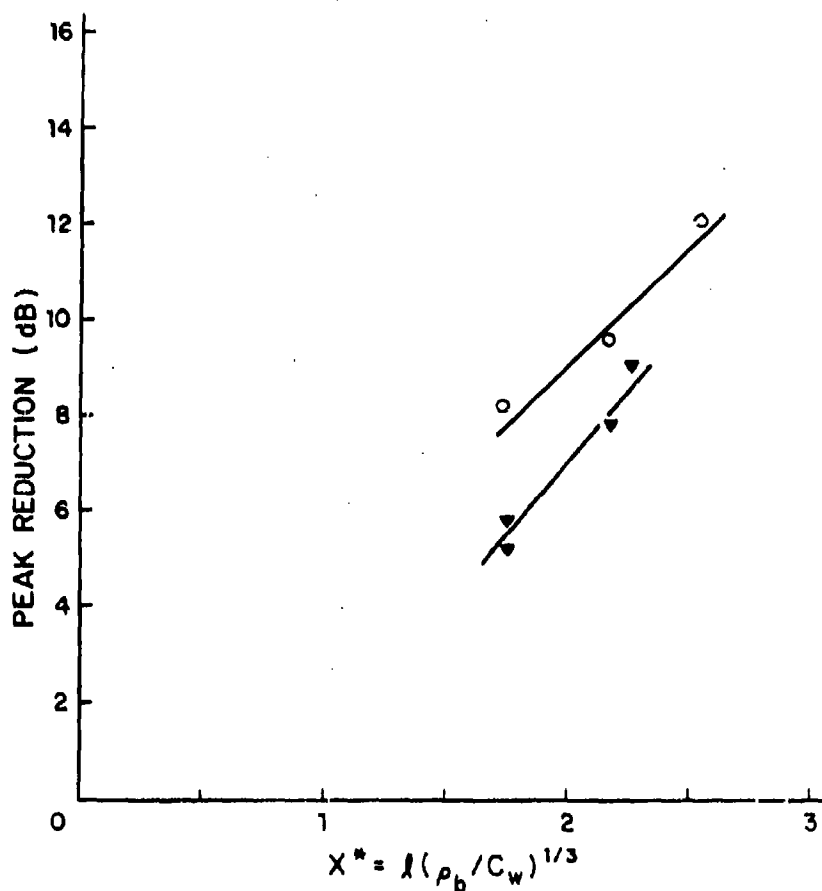


Fig. 4—contd (c)

suffice. Note that this analysis does not exclude surface area from the attenuation model. Surface area viscous effects are still a possible attenuation mechanism.

All test data are combined in Figs 5(a)–(c). Here, the peak level, *FSEL* and *CSEL* reductions are again plotted as a function of the dimensionless material depth X^* . Based on the data presented here, the X^* scaling appears to be a reasonable method for combining data from several materials, quite different in physical properties (see Table 2), loading densities and being driven by different charge weights. However, it is obvious that the scaling is not exact and other material properties should be considered. Of the three metrics, the peak level reduction appears to scale best by the dimensionless X^* . Based on the combined data shown in Figs 5(a)–(c), there is a strong indication that the material mass loading has the strongest influence on blast attenuation.

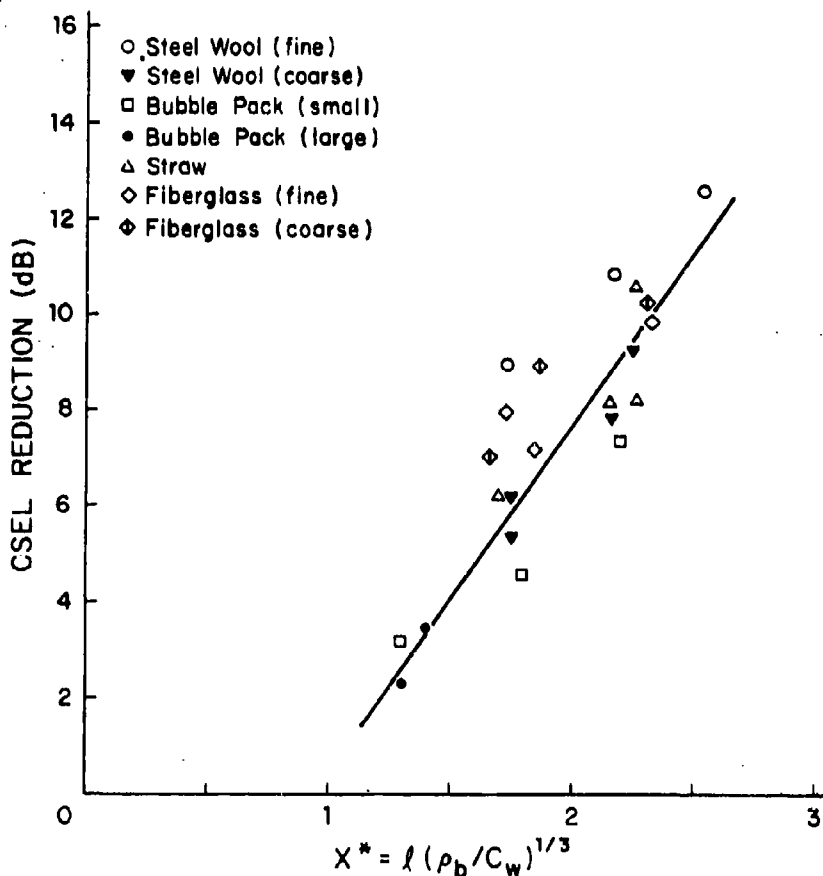


Fig. 5. Noise reductions for all materials scaled to the dimensionless material depth, X^* . (a)

This, however, is limited to the very small range of charge weights considered in these experiments. Further experiments for greater charge masses are needed in order to extrapolate these data beyond a charge weight of 0.57 kg of C-4 explosive.

CONCLUSIONS

The work presented in this paper represents an effort to identify the dominant mechanism for blast wave attenuation in various heterogeneous materials. In all cases the energy source was from detonating either 0.5 or 1 stick of C-4 explosive. All measurements of peak sound level, *FSEL* and *CSEL* were made in the intermediate field environment at either 38 m or 76 m from the energy source. Based on the limited experimental data, the following conclusions are drawn.

Reducing intermediate blast noise

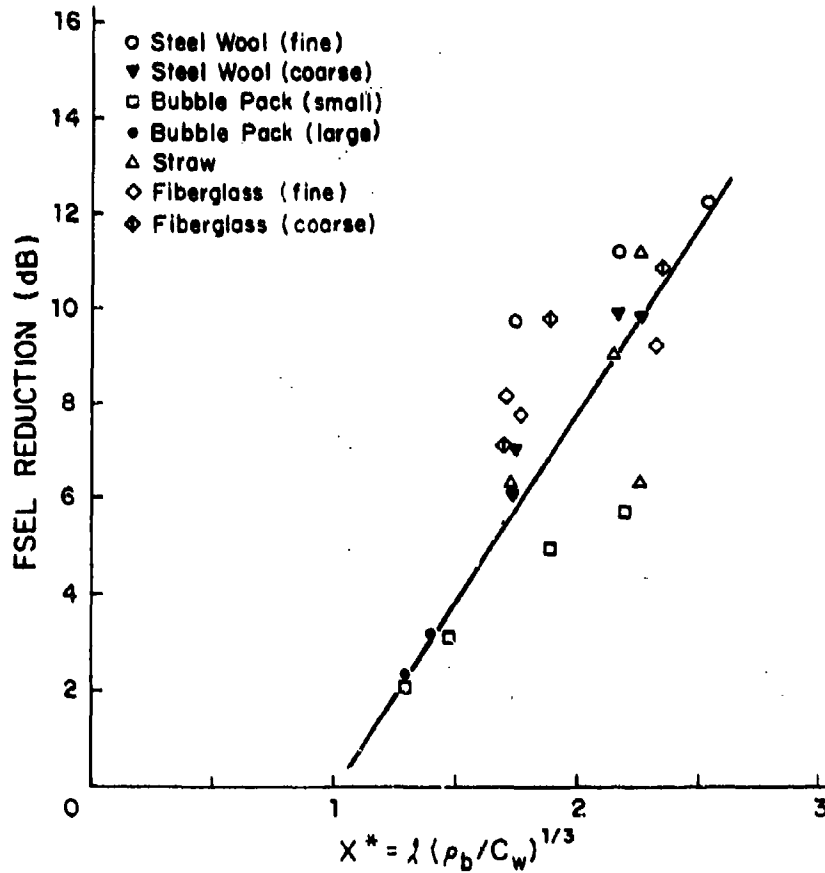


Fig. 5—contd. (b).

First, all four of the materials (steel wool, fiberglass, straw and bubble pack) investigated appeared to scale fairly well with the dimensionless material depth X^* defined in eqn (6). This finding is consistent with previous data presented¹ for blast wave attenuation in aqueous foams. It should be noted, however, that this scaling law should probably not be extrapolated to higher-charge masses without further data to verify the proposed law.

The parameter X^* is a measure of the material mass per charge mass and appears to be the best single scaling parameter available for these types of heterogeneous materials. This is not to imply that other factors such as fiber size and thermal properties of the material do not influence attenuation. Materials that are homogeneous or have very low void fractions would probably not scale according to this law. In all cases studied, the peak level scales more exactly than do the energy integrals *CSEL* and *FSEL*. Although

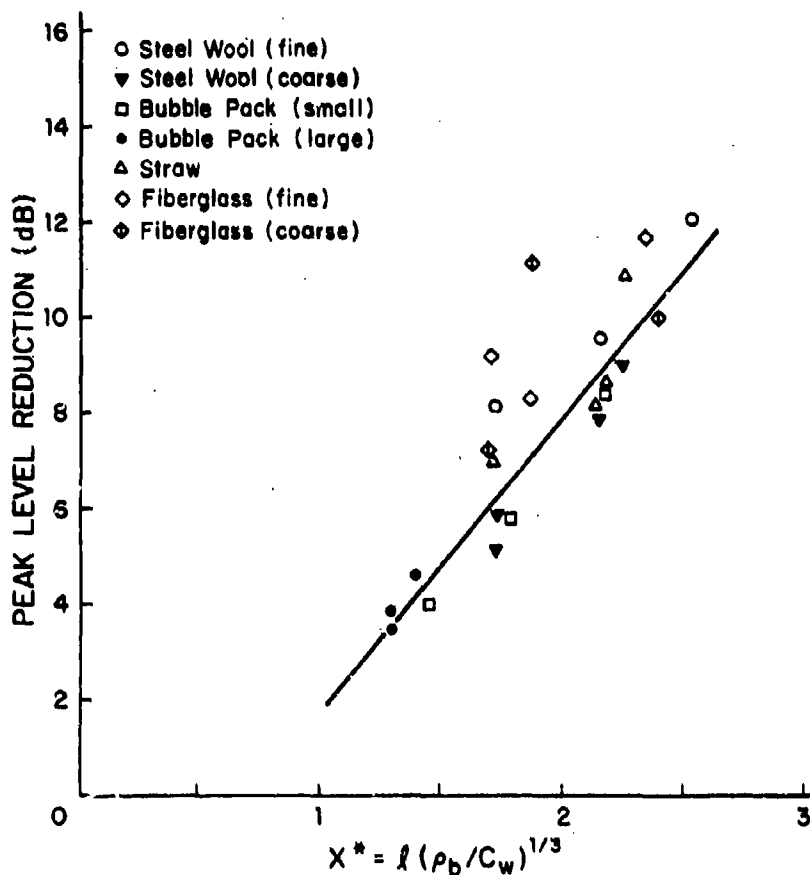


Fig. 5—contd. (c).

the characteristic fiber size (d) influenced the degree of attenuation in some cases, it was not included in the scaling law. The difference in specific surface area between the fiberglass and the steel wool is several orders of magnitude and, as a single parameter, does not describe the relative attenuation difference between samples. If the fiber characteristic length is included in future modeling efforts, it should be in the form of a dimensionless viscous drag term. In this study it was observed that the effect of fiber size is more pronounced for the steel wools than it is for the much finer fiberglass. One possible explanation is that the material fiber size may reach a saturation level where viscous effects are essentially independent of characteristic length.

In conclusion, the data presented provide the basis for engineering estimates of blast wave noise reductions at distances between 38 and 76 m from the source and for charge weights up to 0.57 kg.

REFERENCES

1. R. Ruspet and S. K. Griffiths, The reduction of blast noise with aqueous foam, *J. Acoust. Soc. Am.*, **74**(6) (1983), pp. 1757-63.
2. T. D. Panczak, P. B. Butler and H. Krier, Shock propagation and blast attenuation through aqueous foams, *J. Haz. Mat.*, **14** (1987), pp. 321-36.
3. D. L. Evans, D. F. Jankowski and E. D. Hirtleman, A preliminary investigation of aqueous foam for blast wave attenuation, ERC-R-78050, College of Engineering and Applied Sciences, Arizona State University, Tempe, Arizona, 1979.
4. J. M. Powers and H. Krier, Attenuation of blast waves when detonating explosives inside barriers, *J. Haz. Mat.*, 1985.
5. B. M. Dooratz, *LLNL Explosives Handbook*, University of California, UCRL-52997, 1981.
6. N. Lewis, Personal communication, U.S. Environmental Hygiene Agency.
7. S. K. Griffiths and L. A. Mondy, Internal memo, Sandia National Laboratories, 19 March, 1982.
8. T. D. Panczak and H. Krier, Shock Propagation and Blast Attenuation Through Aqueous Foams, UILU ENG 83-4007, University of Illinois, 1983.
9. Chemical Rubber Company, *Handbook of chemistry and physics*, 1971.

The Reduction of Blast Overpressures from Aqueous Foam in a Rigid Confinement

R. Raspet

US Army Construction Engineering Research Laboratory, Champaign, Illinois (USA)

P. B. Butler and F. Jahani

Department of Mechanical Engineering, The University of Iowa,
Iowa City, Iowa 52242 (USA)

(Received 13 May 1986; revised version received 6 November 1986;
accepted 10 November 1986)

SUMMARY

Experiments were performed in order to quantify the additional attenuation provided by enclosing a blast reducing material (aqueous foam) in a rigid vessel (cylindrical metal culvert), open at one end to the atmosphere. The results are compared with previously reported data on aqueous foam where the culvert was not used. A total of eight configurations were investigated. Tests performed with a 0.91-m culvert section and $\frac{1}{2}$ stick (0.285 kg) of C-4 explosive and with a 1.22-m culvert section with $\frac{1}{2}$ stick and 1 stick of C-4. A third parameter varied in the trials was the amount of foam used (depth in culvert). Data are presented for FSEL, and CSEL and peak level reduction scaled according to a modified scaled foam depth dependent on the charge weight, and height and depth of the culvert. This modified scaling law illustrates the relative effectiveness of enclosure depth and width on the noise reduction.

1 INTRODUCTION

The research discussed in this paper deals primarily with the reduction of blast wave overpressures resulting from detonating high explosives. As reported in previous work,¹⁻⁶ potentially dangerous sound levels can be

mitigated through the use of energy absorbing materials at the blast source. As a continuation of the earlier efforts to understand the reduction of intermediate (i.e. >150dB) noise levels produced by detonating high explosives, the US Army Construction Engineering Research Laboratory (USACERL) has investigated the attenuation levels produced by surrounding an explosive charge with aqueous foam which is confined within a rigid cylindrical vessel. This research is similar to the work reported in Ref. 1 in which the sound absorbing material (aqueous foam) was supported by thin plastic sheeting, an enclosure design which presumably added no additional attenuation.

The experiments reported herein were performed in order to quantify the additional attenuation provided by enclosing the blast reducing material (in this case aqueous foam) in a rigid vessel, open at only one end to the atmosphere. The results are compared with the previously reported data on aqueous foam.¹ Scaling laws will illustrate the relative effectiveness of enclosure depth and width on the level of noise reduction. As in the previous work,^{1,3} the range of charge weights is limited to $0.28 \text{ kg} < C_w < 0.57 \text{ kg}$.

2 EXPERIMENTAL SET-UP

The tests discussed in this paper were conducted at the Fort Leonard Wood, Missouri, demolitions training range. The physical layout of the test facility is similar to the one described by Raspet, Butler and Jahani.³ As in the previous research, Endevco piezo-resistive microphones were mounted on tripods 1.2 m above ground level at various distances from the blast source. In all four microphones were used, two at 38 m from the charge and two at 76 m. Each pair was separated by 90° relative to the blast source. In each test case, three metrics were measured and recorded by the remote data acquisition system. The C-weighted sound exposure level (*CSEL*), the flat-weighted sound exposure level (*FSEL*) and the peak level (*PEAK*) were measured for each of the four stations, and the signals recorded on an Ampex 2230 14-track FM recorder. To assure reliable results, the system was calibrated prior to and after each test using a Bruel & Kjaer piston-phone. By definition, the peak sound pressure level (*PEAK*) and sound exposure level (*SEL*) are given as

$$PEAK(\text{dB}) = 20 \log_{10} [(P_p - P_0)/P_0] \quad (1)$$

$$SEL(\text{dB}) = 10 \log_{10} \left[\int P^2 dt / P_0^2 t_0 \right] \quad (2)$$

where P_p is the peak thermodynamic pressure (Pa), P_0 is a reference pressure ($P_0 = 20 \mu\text{Pa}$), and t_0 is a reference time ($t_0 = 1 \text{ s}$).

Reduction of blast overpressures

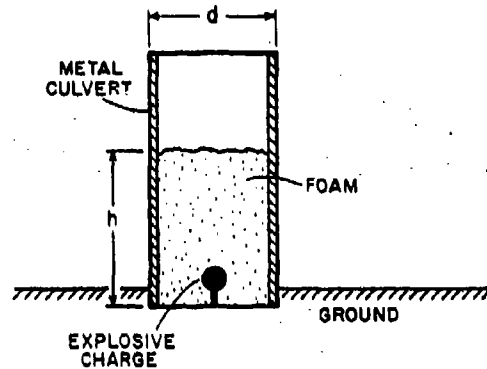


Fig. 1. Schematic of test configuration used in this work. The explosive charge is placed in a metal culvert filled with 30:1 expansion ratio aqueous foam.

All test results described in the following section (see Table 1) were performed with aqueous foam supported by a metal culvert section. This particular configuration is shown in Fig. 1. Two charges were used in each test; a control charge set on a 0.9-m high crushable post, and a test charge set at the center of the cylinder on a 4-cm high post. The culvert sections were sunk into the ground about 6 cm to reduce the propagation of noise under the cylinder. To some extent, this phenomenon did occur since the culvert section was driven into the air by the blast. A total of eight different configurations were investigated. This included tests that were performed with the 0.91-m culvert section and $\frac{1}{2}$ stick (0.285 kg) of C-4, and with a 1.22-m culvert section with $\frac{1}{2}$ stick (0.285 kg) and 1 stick (0.57 kg) of C-4. The third parameter varied in the trials was the amount of foam. In all cases, the experimenters attempted to keep the foam expansion ratio, α , fixed at a value of 30:1 (total volume:liquid volume).

The material referred to as C-4 is a military explosive (91% RDX + 6% TNT + 3% other) with a detonation pressure $P_{CJ} = 25.7$ GPa, detonation velocity $D_{CJ} = 8.4$ mm μs^{-1} and theoretical heat of detonation of $E_{ch} = 5.86$ MJ kg^{-1} .⁷ For comparison, it is about 1.36 times as energetic as TNT.

3 TEST RESULTS

As discussed earlier, the series of tests were performed in order to study the effect of external confinement on the blast reduction produced by aqueous foams. A schematic of the test configuration is shown in Fig. 1. The confining vessel is a cylindrical metal culvert, open at the top end. During all tests, the explosive charge was first set in the test cylinder and then the cylinder was

TABLE 1
Test Data and Scaled Foam Depths

| Test number | Explosive mass (kg) | <i>d</i> (m) | <i>h</i> (m) | $\Delta PEAK$ | $\Delta CSEL$ (dB) | $\Delta FSEL$ (dB) | \hat{X} | \bar{X} |
|-------------|---------------------|--------------|--------------|---------------|--------------------|--------------------|-----------|-----------|
| 101a | 0.28 | 0.92 | 0.86 | 20.6 | 18.5 | 17.8 | 0.71 | 3.75 |
| 101b | 0.28 | 0.92 | 0.55 | 16.8 | 14.4 | 14.0 | 0.61 | 2.77 |
| 102a | 0.28 | 1.22 | 1.16 | 24.9 | 21.6 | 19.4 | 0.95 | 4.99 |
| 102b | 0.28 | 1.22 | 0.86 | 23.3 | 22.2 | 20.8 | 0.86 | 4.09 |
| 102c | 0.28 | 1.22 | 0.55 | 18.0 | 15.8 | 15.1 | 0.74 | 3.04 |
| 103a | 0.57 | 1.22 | 1.16 | 22.0 | 20.4 | 19.8 | 0.75 | 3.96 |
| 103b | 0.57 | 1.22 | 0.86 | 21.1 | 19.8 | 19.2 | 0.68 | 3.25 |
| 103c | 0.57 | 1.22 | 0.55 | 16.1 | 14.4 | 14.3 | 0.59 | 2.41 |

any differences in a quantitative manner, it is necessary to apply scaling laws to these data.

4 DISCUSSION OF RESULTS

These tests were performed so that the scaling laws developed in Raspet and Griffiths¹ could be applied to cases where the foam is supported by rigid walls. Data presented in Ref. 1, where unconfined aqueous foam was used as the blast reducing agent, indicated that a scaled foam depth

$$\hat{X} = l(C_w^{1/3}) \quad (4a)$$

scaled foams of the same density, and that a dimensionless foam depth defined as

$$X = l(\rho_f/C_w)^{1/3} \quad (4b)$$

scaled foams of different densities quite well. In eqns (4), ρ_f represents the foam density, l represents the geometrically averaged pit depth (see Fig. 2), and C_w is the mass of explosive in equivalent kilograms of TNT. This is also the same form of the scaling used in Ref. 3, where fiberglass, steel wool and other materials were used in place of foam. Since all the experiments reported in Refs 1 and 3 were for the cubic arrangement shown in Fig. 2, the geometrically averaged foam depth was given as

$$l = \frac{1}{2}a \quad (5)$$

where a is the dimension of the cube shown in Fig. 2.

Because the current experimental layout is somewhat similar to that

reported in Refs 1 and 3, and because the observed trends are also similar, a scaling law such as eqn (4b) is a prime candidate for these new data.

Before this can be accomplished, a reasonable way of adjusting for charges at the bottom of the foam volume, rather than centered in the volume, must be developed. Theoretically, there are two counteracting effects. First, the energy from the charge propagates into a solid angle of 2π rather than 4π , thus increasing the effective charge by a factor of two. Second, energy is absorbed by the ground, which results in a reduction of the effective charge weight. We can use the results of two experimental tests to guide us in choosing an effective weight. Tests at Fort Leonard Wood in conjunction with earlier tests⁸ indicated that charges on the ground were quieter by 3 dB *FSEL*.

Measurements of the sound level reduction from charges set in the culvert with no blast noise reducing materials are given in Table 2. It is interesting to

TABLE 2
Reductions with No Foam in Culvert

| <i>Metric</i> | <i>d</i> (<i>m</i>) | <i>Reduction</i> (<i>dB</i>) |
|---------------|--------------------------|-----------------------------------|
| <i>PEAK</i> | 0.91 | -0.3 |
| <i>FSEL</i> | 0.91 | 1.0 |
| <i>CSEL</i> | 0.91 | 1.0 |
| <i>PEAK</i> | 1.22 | 1.3 |
| <i>FSEL</i> | 1.22 | 2.5 |
| <i>CSEL</i> | 1.22 | 2.5 |

note that the system of culvert plus ground has a larger reduction on the energy measures than on the peak levels. This indicates that the dissipation in this case is possibly due to multiple reflections after the initial shock front develops. In view of the variation in data and the sparsity of data, the best adjustment is the simplest. We will use the geometrically averaged foam depth divided by the cube root of the charge weight. This is equivalent to assuming that half the energy of the charge is propagated into the ground. We will scale the data using this simple model and note any variations which might be caused by this particular choice.

For comparison with the previous data, the scaled foam depths (\hat{X}) for each of the current tests are listed in Table 1. The *CSEL* reduction versus scaled foam depth is displayed in Fig. 3a, the *FSEL* reduction in Fig. 3b and the peak reduction in Fig. 3c. Also displayed on these figures are the lines fitted to the unconfined data in Ref. 1.

For the cylindrical geometry of the culvert, the characteristic foam depth /

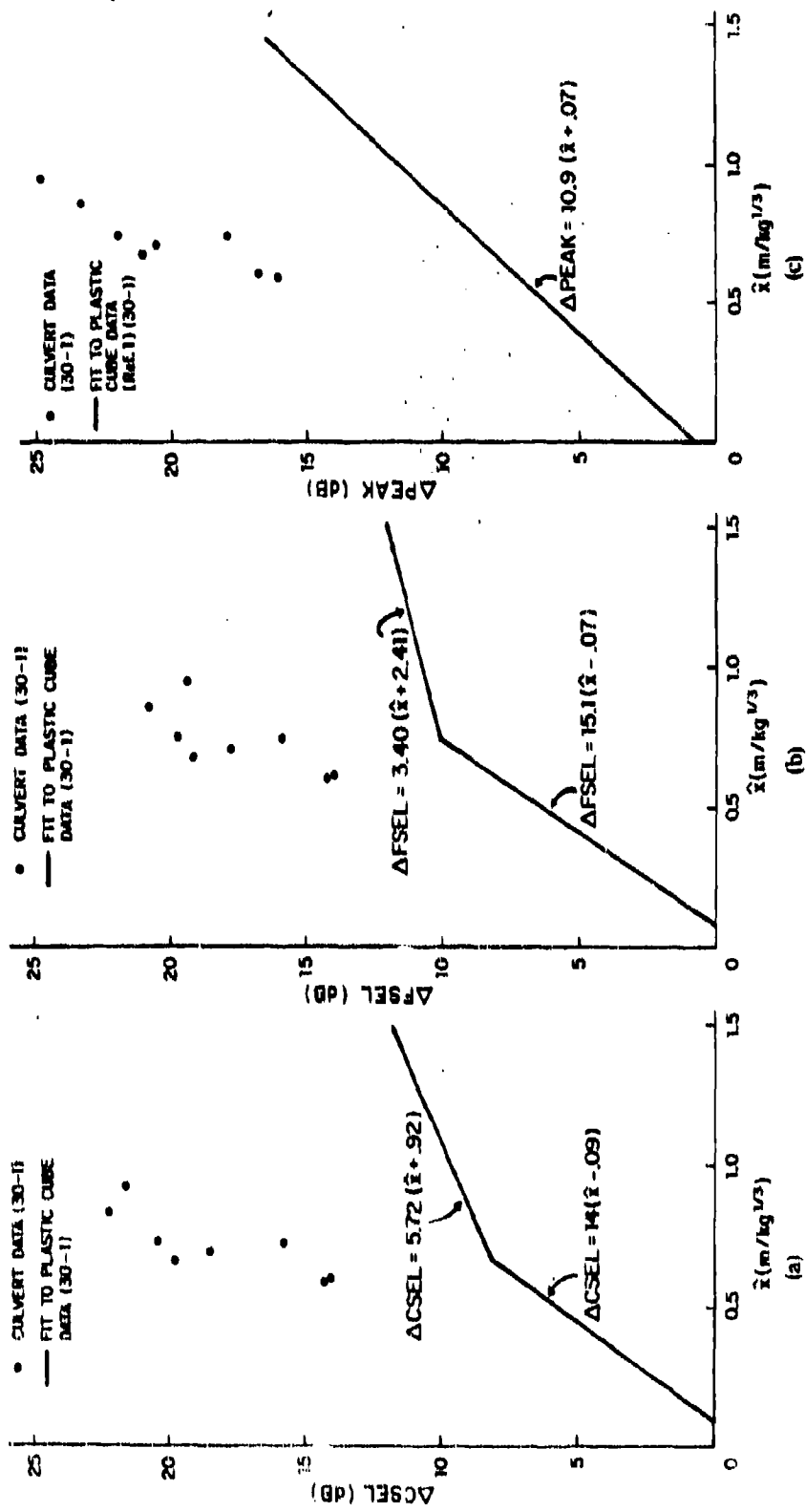


Fig. 3. (a) CSEL reduction scaled to foam depth \bar{x} as defined in Ref. 1. (b) Scaled FSEL reduction: the solid line represents the data from Ref. 1. where the foam is confined in a plastic cube. (c) Peak level reduction scaled to foam depth \bar{x} .

is given as the equivalent radius of a sphere with the same volume as the cylinder. That is,

$$l = (\frac{3}{16}d^2h)^{1/3} \quad (6)$$

Obviously, these tests are not extensive enough to provide detailed scaling laws giving reduction as a function of diameter, depth and charge size. However, these tests do provide an engineering estimate of the reduction produced by confined charges.

A notable feature of this data is the tendency of the dB reduction to saturate for the larger depths. There is a large change in reduction from 0.55 to 0.86 m depth, and a smaller change in reduction from 0.86 to 1.16 m depth. Since the foam is unconfined in the vertical directions, perhaps vertical saturation is beginning to occur at these depths.

It appears that equivalent depth variations produce larger changes than equivalent diameter variations. That is, if the foam volume is kept constant so that the scaled foam depth is constant but the depth increased and diameter decreased, the reduction will increase. A more accurate theory may need to divide the volume dependence of scaling into an area dependence and a depth dependence.

Figures 4a, b and c show the *FSEL* reduction, *CSEL* reduction and peak level reduction plotted as a function of a modified scaled foam depth X , defined as

$$X = A^{1/6}h^{2/3}(\rho_f/C_w)^{1/3} \quad (7)$$

where A is the surface area of foam and h is the depth of foam. The scaled data shows good agreement, with the exception of one erroneous data point (103b). When one excludes this data point along with the data point that appears to be in the saturation region, a linear regression analysis gives reasonable results. These are displayed in Table 3 for all three metrics. Here the reductions are 4.17, 4.05 and 4.54 dB/scaled distance for *PEAK*, *FSEL* and *CSEL*, respectively.

TABLE 3
Linear Regression Calculations for Experimental Data Less 102a and 103b: $Y = AX + B$

| Variable Y (dB) | Correlation coefficient | A | B |
|----------------------|----------------------------|------|------|
| $\Delta PEAK$ | 0.99 | 4.17 | 5.53 |
| $\Delta FSEL$ | 0.96 | 4.05 | 3.44 |
| $\Delta CSEL$ | 0.96 | 4.54 | 2.43 |

Reduction of blast overpressures

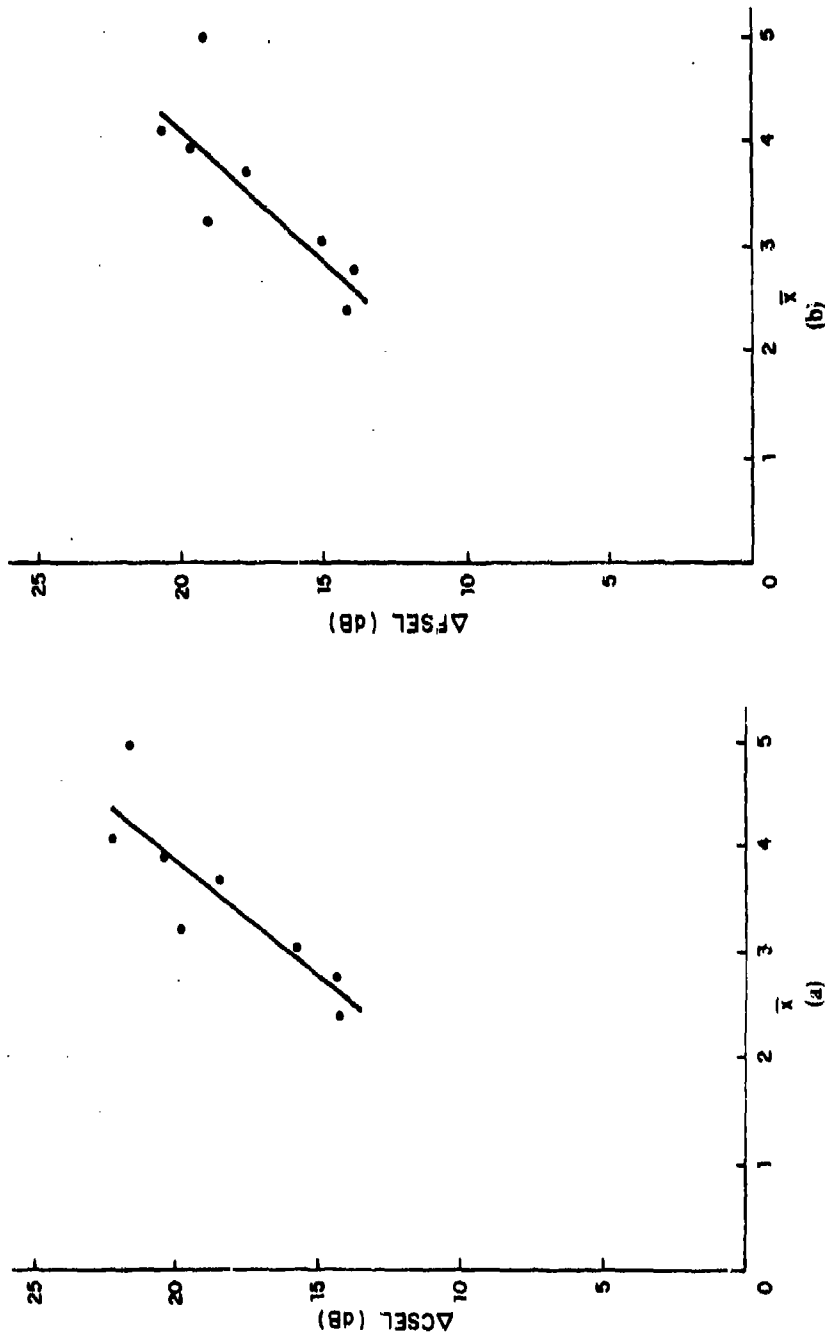


Fig. 4. (a) CSEL reduction scaled to $X = A^{1/3} \rho_0^{2/3} (\rho_0 / C_0)^{1/3}$. (b) FSEL reduction for aqueous foam confined within a metal culvert: X is defined in Fig. 4a.

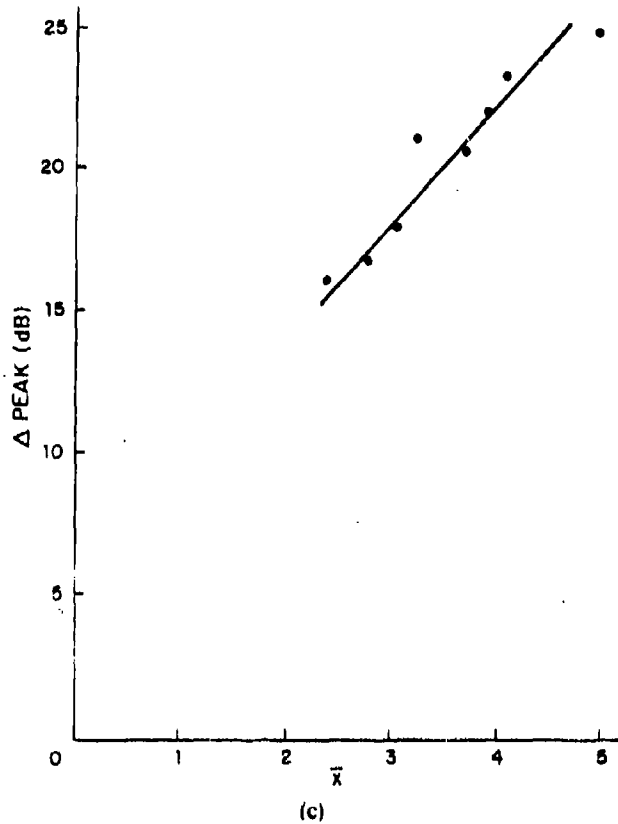


Fig. 4. (c) Peak level reductions for aqueous foam in a metal culvert.

5 CONCLUSIONS

In this work, we have investigated the attenuation effectiveness of aqueous foam confined in a rigid metal structure. When compared to previous data¹ for unconfined foam, it appears that the rigid confinement contributes to the attenuation process. It may be that the wave reflections off the internal walls, as well as the heterogeneous medium, dissipate energy. Previous data¹ showed that, for the unconfined case, the dimensionless material (foam) depth provided a reasonable scaling law. For the confined situation, it was shown that for several different configurations the best scaling was with foam depth raised to the $\frac{2}{3}$ power and surface area to the $\frac{1}{6}$ power in addition to the regular charge mass to the $-\frac{1}{3}$ power. The system of culvert plus ground has a larger reduction in the energy levels than in the peak levels. This indicates that the dissipation in this case is due to multiple reflections

Reduction of blast overpressures

after the initial shock front develops. This is consistent with the wave reflection statement made above.

It should also be noted that the geometrical arrangement provided in these tests results in a focusing of the blast energy in the vertical direction. The degree of attenuation provided at distances greater than 76 m can only be determined by measurements, since it is not clear if the readings at 76 m are affected by this energy.

REFERENCES

1. R. Raspet and S. K. Griffiths, The reduction of blast noise with aqueous foam, *J. Acoust. Soc. Am.*, **74**(6) (1983), pp. 1757-63.
2. T. D. Panczak, P. B. Butler and H. Krier, Shock propagation and blast attenuation through aqueous foams, *J. Haz. Mat.*, **14** (1987), pp. 321-36.
3. R. Raspet, P. B. Butler and F. Jahani, The effect of material properties on reducing intermediate blast noise, *Applied Acoustics*, **22**(4) (1987).
4. J. M. Powers and H. Krier, Attenuation of blast waves when detonating explosives inside barriers, *J. Haz. Mat.*, **13** (1986), pp. 121-33.
5. T. D. Panczak and H. Krier, *Shock propagation blast attenuation through aqueous foams*, UILU ENG 83-4003, Urbana, Illinois, 1983.
6. D. L. Evans, D. F. Jankowski and E. D. Hirleman, *A preliminary investigation of aqueous foam for blast wave attenuation*, ERC-R-78050, College of Engineering and Applied Sciences, Arizona State University, Tempe, Arizona, 1979.
7. B. M. Dobratz, *LLNL explosive handbook*, UCRL-52997, University of California, 1981.
8. P. D. Schomer, R. J. Goff and L. M. Little, *The statistics of amplitude and spectrum of blast propagated in the atmosphere*, CERL Report N-13, US Army Construction Engineering Research Laboratory, Champaign, Ill., 1976.

ENA Team Distribution

Chief of Engineers

ATTN: CEEC-CE

ATTN: CEEC-EA

ATTN: CEEC-EI (2)

ATTN: CEEC-ZA

ATTN: CEEC-M (2)

HQ USAF/LEEEU 20332

AMC 22333

ATTN: AMCEN-A

Naval Air Systems Command 20360

ATTN: Library

Little Rock AFB 72099

ATTN: 314/DEEE

Aberdeen PG, MD 21010

ATTN: Safety Office Range Safety Div.

ATTN: U.S. Army Ballistic Research Lab (2)

ATTN: ARNG Operating Activity Ctr.

35

+40

11/88

Edgewood Arsenal, MD 21010

ATTN: HSHB-MO-B

Ft. Belvoir, VA 22060

ATTN: NACEC-FB

NAVFAC 22332

ATTN: Code 2003

Naval Surface Weapons Center 22448

ATTN: N-43

Ft. McPherson, GA 30330

ATTN: AFEN-FEB

US Army Aeromedical Res Lab. 36362

ATTN: SGRD-UAS-AS

USA-WES 39180

ATTN: WESSEN-B

ATTN: Soils & Pavements Lab

ATTN: C/Structures

Wright-Patterson AFB, OH 45433

ATTN: AAMRL/BB

ATTN: AAMRL/BBE

Human Engr. Laboratory 21010

Naval Undersea Center, Code 401 92132

Bureau of National Affairs 20037

Building Research Board 20418

Transportation Research Board 20418

Department of Transportation

ATTN: Library 20590

Federal Aviation Administration 20591

Defense Technical Info Ctr

ATTN: DDA (2)